Applications of Mathematics

Dalibor Lukáš

On solution to an optimal shape design problem in 3-dimensional linear magnetostatics

Applications of Mathematics, Vol. 49 (2004), No. 5, 441–464

Persistent URL: http://dml.cz/dmlcz/134578

49 (2004) APPLICATIONS OF MATHEMATICS No. 5, 441–464

ON SOLUTION TO AN OPTIMAL SHAPE DESIGN PROBLEM IN 3-DIMENSIONAL LINEAR MAGNETOSTATICS*

DALIBOR LUKÁŠ, Ostrava

(Received September 9, 2002, in revised version January 15, 2004)

Abstract. In this paper we present theoretical, computational, and practical aspects concerning 3-dimensional shape optimization governed by linear magnetostatics. The state solution is approximated by the finite element method using Nédélec elements on tetrahedra. Concerning optimization, the shape controls the interface between the air and the ferromagnetic parts while the whole domain is fixed. We prove the existence of an optimal shape. Then we state a finite element approximation to the optimization problem and prove the convergence of the approximated solutions. In the end, we solve the problem for the optimal shape of an electromagnet that arises in the research on magnetooptic effects and that was manufactured afterwards.

Keywords: optimal shape design, finite element method, magnetostatics, magnetooptics

MSC 2000: 49J20, 65K10, 35J40, 65N30

1. INTRODUCTION

In the paper we present 3-dimensional (3d) shape optimization of an electromagnet arising in the research on magnetooptic effects. A useful framework for the existence and convergence proofs is given by an abstract theory in [11] together with applications mostly in mechanics. Our theory differs mainly by the fact that the optimized shape controls the interface between the air and the ferromagnetic parts, rather than the whole domain boundary, as it is usual in mechanics. The domain is fixed in our

* This research has been supported by the Austrian Science Fund FWF within the SFB "Numerical and Symbolic Scientific Computing" under grant SFB F013, by the Czech Ministry of Education under research project CEZ: J17/98:272400019, and by the Grant Agency of the Czech Republic under grant 105/99/1698.

case. Variational formulations of the magnetostatic problem and their finite element discretizations are given in [2], [14], [30] using the space $\mathbf{H(curl)}$ that was well described in [7], [22]. Some shape optimization problems governed by 2-dimensional (2d) nonlinear magnetostatics are treated in [23], [29].

The paper is organized as follows. In Section 2 we introduce a weak formulation of linear magnetostatics in $\mathbf{H_0(curl)}/\mathbf{Ker_0(curl)}$ and prove the existence and uniqueness of the solution. Further, we regularize the bilinear form due to its nonellipticity and prove the convergence of the regularized solutions. Finally, we discretize the problem by the finite element method using the first-order Nédélec tetrahedral elements and prove the convergence. In Section 3 we introduce a shape optimization problem. We prove the compactness of the set of admissible shapes and the continuity of the cost functional. We regularize the bilinear form, employ the finite element discretization, and prove the convergence of the optimized discretized shapes. Finally, we make notes on the first-order sensitivity analysis. In Section 4 the theory is applied to optimal shape design of an electromagnet. We give a 3d optimized shape as well as a 2d one which resulted from a dimensionally reduced formulation. According to the 2d optimized shape, pole heads of the electromagnet were manufactured and we discuss the improvements in terms of physical measurements of the magnetic field before and after optimization.

2. Three-dimensional linear magnetostatics

Assumption 1. In all what follows let $\Omega \subset \mathbb{R}^3$ be a nonempty bounded convex domain with a polyhedral boundary.

2.1. Linear magnetostatics

Let $\mathbf{B}$ and $\mathbf{J}$ denote the magnetic field and the current density, respectively. We introduce the magnetic vector potential $\mathbf{u}$ by

$$\mathbf{curl}(\mathbf{u}) = \mathbf{B}.$$

We consider the following magnetostatic boundary value problem:

$$\text{(S)} \qquad \begin{cases} \mathbf{curl}\Big(\dfrac{1}{\mu}\,\mathbf{curl}(\mathbf{u})\Big) = \mathbf{J} & \text{in } \Omega \\ \mathbf{n} \times \mathbf{u} = \mathbf{0} & \text{on } \partial\Omega \end{cases}$$

We suppose that only the air and the ferromagnetics occupy Ω, i.e., there exists a decomposition of Ω into subdomains Ω_0 and Ω_1 such that

$$\overline{\Omega} = \overline{\Omega_0} \cup \overline{\Omega_1}, \quad \Omega_0 \cap \Omega_1 = \emptyset, \quad \text{and} \quad \mathrm{meas}(\Omega_0), \mathrm{meas}(\Omega_1) \neq 0,$$

where meas stands for the Lebesgue measure and we suppose that there exist constants μ_0, μ_1 such that

$$0 < \mu_0 < \mu_1, \quad \mu|_{\Omega_0} = \mu_0, \quad \text{and} \quad \mu|_{\Omega_1} = \mu_1. \tag{1}$$

2.2. The space H(curl)

We will extend the differential operator **curl** to a subspace of $[L^2(\Omega)]^3$. A function $\mathbf{z} \in [L^2(\Omega)]^3$ is called the *generalized rotation* of $\mathbf{u} \in [L^2(\Omega)]^3$ if

$$\forall \mathbf{v} \in [C_0^\infty(\Omega)]^3 : \int_\Omega \mathbf{u} \cdot \mathbf{curl}(\mathbf{v})\, \mathbf{dx} = \int_\Omega \mathbf{z} \cdot \mathbf{v}\, \mathbf{dx}$$

and we denote the generalized rotation by $\mathbf{curl}(\mathbf{u}) := \mathbf{z}$. We define the space

$$\mathbf{H}(\mathbf{curl}; \Omega) := \{\mathbf{u} \in [L^2(\Omega)]^3 \mid \exists \mathbf{z} \in [L^2(\Omega)]^3 : \ \mathbf{z} = \mathbf{curl}(\mathbf{u})\}$$

which together with the scalar product

$$(\mathbf{u}, \mathbf{v})_{\mathbf{curl},\Omega} := \int_\Omega \mathbf{u} \cdot \mathbf{v}\, \mathbf{dx} + \int_\Omega \mathbf{curl}(\mathbf{u}) \cdot \mathbf{curl}(\mathbf{v})\, \mathbf{dx}$$

forms a Hilbert space. We introduce the induced norm and seminorm by

$$\|\mathbf{u}\|_{\mathbf{curl},\Omega} := \sqrt{(\mathbf{u}, \mathbf{u})_{\mathbf{curl},\Omega}} \quad \text{and} \quad |\mathbf{u}|_{\mathbf{curl},\Omega} := \sqrt{\int_\Omega \|\mathbf{curl}(\mathbf{u})\|^2\, \mathbf{dx}},$$

where $\|\cdot\|$ denotes the Euclidean norm.

Due to [7, p. 34], the operator $\mathbf{n} \times \mathbf{u}|_{\partial\Omega}$ can be extended by continuity onto the space $\mathbf{H}(\mathbf{curl}; \Omega)$. Thus, the following spaces are well-defined:

$$\mathbf{H_0}(\mathbf{curl}; \Omega) := \{\mathbf{u} \in \mathbf{H}(\mathbf{curl}; \Omega) \mid \mathbf{n} \times \mathbf{u} = \mathbf{0} \text{ on } \partial\Omega\},$$
$$\mathbf{Ker_0}(\mathbf{curl}; \Omega) := \{\mathbf{u} \in \mathbf{H_0}(\mathbf{curl}; \Omega) \mid \mathbf{curl}(\mathbf{u}) = \mathbf{0} \text{ in } \Omega\}.$$

The quotient space $\mathbf{H_0}(\mathbf{curl}; \Omega)/\mathbf{Ker_0}(\mathbf{curl}; \Omega)$ will be used as the test space for a weak formulation of (S). By [12, p. 94–95] it is isomorphically isometric to

$$\mathbf{H_{0,\perp}}(\mathbf{curl}; \Omega) := \left\{\mathbf{u} \in \mathbf{H_0}(\mathbf{curl}; \Omega) \mid \forall p \in H_0^1(\Omega) : \int_\Omega \mathbf{u} \cdot \mathbf{grad}(p)\, \mathbf{dx} = 0\right\}.$$

Moreover, we have the orthogonal decomposition

$$\mathbf{H_0}(\mathbf{curl}; \Omega) = \mathbf{H_{0,\perp}}(\mathbf{curl}; \Omega) \oplus \mathbf{Ker_0}(\mathbf{curl}; \Omega).$$

The following densities hold in the norm $\|\cdot\|_{\mathbf{curl},\Omega}$:

$$\mathbf{H}(\mathbf{curl}; \Omega) = \overline{[C^\infty(\overline{\Omega})]^3} \quad \text{and} \quad \mathbf{H_0}(\mathbf{curl}; \Omega) = \overline{[C_0^\infty(\Omega)]^3}. \tag{2}$$

Finally, we will make use of a Friedrichs'-like inequality:

Lemma 1. *There exists a positive constant C_1 such that*

$$\forall\, \mathbf{v} \in \mathbf{H_{0,\perp}(curl;\Omega)}\colon\ \|\mathbf{v}\|_{\mathbf{curl},\Omega} \leqslant C_1 |\mathbf{v}|_{\mathbf{curl},\Omega}.$$

Proof. See [12, p. 96]. □

2.3. Weak formulation

We introduce a bilinear form a and a linear functional f, both related to (S), by

$$a(\mathbf{v},\mathbf{u}) := \int_{\Omega_0} \frac{1}{\mu_0}\mathbf{curl}(\mathbf{v})\cdot\mathbf{curl}(\mathbf{u})\,\mathrm{d}\mathbf{x} + \int_{\Omega_1} \frac{1}{\mu_1}\mathbf{curl}(\mathbf{v})\cdot\mathbf{curl}(\mathbf{u})\,\mathrm{d}\mathbf{x},$$
$$f(\mathbf{v}) := \int_\Omega \mathbf{J}\cdot\mathbf{v}\,\mathrm{d}\mathbf{x}, \quad \mathbf{u},\mathbf{v} \in \mathbf{H(curl;\Omega)},$$

where the current density $\mathbf{J} \in [L^2(\Omega)]^3$ satisfies the compatibility condition

$$(3)\quad \forall\, \mathbf{w} \in \mathbf{Ker_0(curl;\Omega)}\colon\ f(\mathbf{w}) = 0, \quad \text{i.e.,} \quad \forall\, p \in H_0^1(\Omega)\colon \int_\Omega \mathbf{J}\cdot\mathbf{grad}(p)\,\mathrm{d}\mathbf{x} = 0.$$

Then, the weak formulation of (S) reads as follows:

$$(\mathrm{W}) \qquad \begin{cases} \text{Find } \mathbf{u} \in \mathbf{H_{0,\perp}(curl;\Omega)}\colon \\ a(\mathbf{v},\mathbf{u}) = f(\mathbf{v})\ \ \forall\, \mathbf{v} \in \mathbf{H_{0,\perp}(curl;\Omega)}. \end{cases}$$

Lemma 2. *There exists a unique solution $\mathbf{u} \in \mathbf{H_{0,\perp}(curl;\Omega)}$ to* (W).

Proof. It is easy to see that the space $\mathbf{H_{0,\perp}(curl;\Omega)}$ equipped with the scalar product $(\cdot,\cdot)_{\mathbf{curl},\Omega}$ forms a Hilbert space and that the linear functional f and the bilinear form a are bounded. The ellipticity of a on $\mathbf{H_{0,\perp}(curl;\Omega)}$ follows from

$$(4)\qquad a(\mathbf{v},\mathbf{v}) \geqslant \frac{1}{\mu_1}\int_\Omega \|\,\mathbf{curl}(\mathbf{v})\|^2\,\mathrm{d}\mathbf{x} = \frac{1}{\mu_1}|\mathbf{v}|^2_{\mathbf{curl},\Omega} \geqslant \frac{1}{\mu_1 C_1^2}\|\mathbf{v}\|^2_{\mathbf{curl},\Omega},$$

where we have used (1) and Lemma 1. The statement now follows directly from the Lax-Milgram lemma, cf. [14, p. 14]. □

2.4. Regularization of the bilinear form

The problem (W) is equivalent to a mixed variational formulation. We will rather introduce a non-mixed formulation in $\mathbf{H_0(curl;\Omega)}$ while we regularize the nonellipticity of a. The solutions will then tend towards the solution of (W).

Let $\varepsilon > 0$ be a regularization parameter by which we regularize a:

$$a_\varepsilon(\mathbf{v}, \mathbf{u}) := a(\mathbf{v}, \mathbf{u}) + \varepsilon \int_\Omega \mathbf{v} \cdot \mathbf{u} \, \mathrm{d}\mathbf{x}, \quad \mathbf{u}, \mathbf{v} \in \mathbf{H}(\mathbf{curl}; \Omega).$$

The regularized weak formulation then reads

$$(\mathrm{W}_\varepsilon) \qquad \begin{cases} \text{Find } \mathbf{u}_\varepsilon \in \mathbf{H_0}(\mathbf{curl}; \Omega): \\ a_\varepsilon(\mathbf{v}, \mathbf{u}_\varepsilon) = f(\mathbf{v}) \quad \forall \mathbf{v} \in \mathbf{H_0}(\mathbf{curl}; \Omega), \end{cases}$$

where we still assume that (3) holds.

For each $\varepsilon > 0$ we can easily prove the existence of a unique solution $\mathbf{u}_\varepsilon$ to (W_ε). The following lemma gives a convergence property:

Lemma 3. *The following convergence holds:*

$$\mathbf{u}_\varepsilon \to \mathbf{u} \text{ in } \mathbf{H_0}(\mathbf{curl}; \Omega) \text{ as } \varepsilon \to 0_+,$$

where $\mathbf{u}_\varepsilon$ *are the solutions to* (W_ε) *and* $\mathbf{u}$ *is the solution to* (W).

Proof. See [27, Lemma 2.1]. □

2.5. Finite element approximation

We denote by $\mathcal{T}^h := \{K^{e_i} \mid i = 1, \ldots, n_\Omega\}$ a face-to-face discretization of Ω into tetrahedra. Let h^e denote the length of the shortest edge of a tetrahedron K^e. We denote by $h := \min_{K^e \in \mathcal{T}^h} h^e$ the discretization parameter. Clearly, there exists $\overline{h} > 0$ being the maximal size in the geometry such that $h \leqslant \overline{h}$.

2.5.1. Discretization of the test space using Nédélec elements

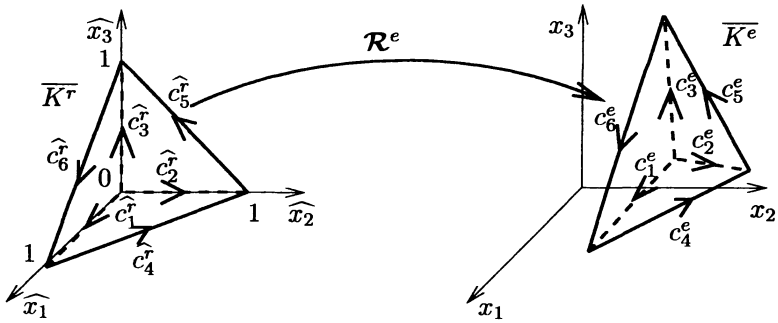

Figure 1. A transformation from the reference Nédélec tetrahedron.

The *linear Nédélec element* is a triple $E := (\overline{K^e}, \mathbf{P}^e, \Sigma^e)$, where $K^e \subset \mathbb{R}^3$ is a tetrahedral domain,

$$\mathbf{P}^e := \{\mathbf{p}(\mathbf{x}) := \mathbf{a}^e \times \mathbf{x} + \mathbf{b}^e \mid \mathbf{a}^e, \mathbf{b}^e \in \mathbb{R}^3,\ \mathbf{x} := (x_1, x_2, x_3) \in \overline{K^e}\},$$

and $\Sigma^e := \{\sigma_1^e, \ldots, \sigma_6^e\}$, where the degree of freedom is defined by

$$\sigma_i^e(\mathbf{v}) := \int_{c_i^e} \mathbf{v} \cdot \mathbf{t}_i^e \, \mathrm{ds}, \quad i = 1, \ldots, 6,$$

where c_i^e stand for oriented edges, see Fig. 1, and $\mathbf{t}_i^e$ are the related unit tangential vectors. By [22, Th. 1], this element is $\mathbf{H}(\mathbf{curl}; K^e)$-conforming.

By $\boldsymbol{\xi}_1^e, \ldots, \boldsymbol{\xi}_6^e \in \mathbf{P}^e$ we denote the shape functions related to the element K^e. In a standard way we introduce the global shape functions $\boldsymbol{\xi}_1^h, \ldots, \boldsymbol{\xi}_n^h \colon \overline{\Omega} \mapsto \mathbb{R}^3$, where n is the number of edges (degrees of freedom) in the discretization $\mathcal{T}^h$. We introduce a conforming approximation of $\mathbf{H_0}(\mathbf{curl}; \Omega)$ by

$$\mathbf{H_0}(\mathbf{curl}; \Omega)^h := \left\{ \mathbf{v}^h = \sum_{\mathbf{n} \times \boldsymbol{\xi}_i^h = \mathbf{0}} v_i^h \boldsymbol{\xi}_i^h \mid v_i^h \in \mathbb{R} \right\}.$$

It can be easily seen that $\mathbf{H_0}(\mathbf{curl}; \Omega)^h \subset \mathbf{H_0}(\mathbf{curl}; \Omega)$, see [17].

The linear transformation $\mathcal{R}^e(\hat{\mathbf{x}}) := \mathbf{R}^e \cdot \hat{\mathbf{x}} + \mathbf{r}^e$ in Fig. 1 is determined by

$$\mathbf{R}^e := \begin{pmatrix} x_{2,1}^e - x_{1,1}^e & x_{3,1}^e - x_{1,1}^e & x_{4,1}^e - x_{1,1}^e \\ x_{2,2}^e - x_{1,2}^e & x_{3,2}^e - x_{1,2}^e & x_{4,2}^e - x_{1,2}^e \\ x_{2,3}^e - x_{1,3}^e & x_{3,3}^e - x_{1,3}^e & x_{4,3}^e - x_{1,3}^e \end{pmatrix}, \quad \mathbf{r}^e := \begin{pmatrix} x_{1,1}^e \\ x_{1,2}^e \\ x_{1,3}^e \end{pmatrix},$$

where $\mathbf{x}_i^e := (x_{i,1}^e, x_{i,2}^e, x_{i,3}^e)$, $i = 1, \ldots, 4$, are the corners of the tetrahedron $\overline{K^e}$ which correspond to the corners of $\overline{K^r}$:

$$\widehat{\mathbf{x}_1^r} := (0,0,0), \quad \widehat{\mathbf{x}_2^r} := (1,0,0), \quad \widehat{\mathbf{x}_3^r} := (0,1,0), \quad \widehat{\mathbf{x}_4^r} := (0,0,1).$$

The following Piola's transformation holds, see [26, Form. 3.17]:

$$\mathbf{curl}_{\mathbf{x}}(\mathbf{v}(\mathbf{x})) = \frac{1}{\det(\mathbf{R}^e)} \mathbf{R}^e \cdot \mathbf{curl}_{\hat{\mathbf{x}}}(\hat{\mathbf{v}}(\hat{\mathbf{x}})), \tag{5}$$

where $\mathbf{v}(\mathbf{x})$ and $\hat{\mathbf{v}}(\hat{\mathbf{x}})$ respectively stand for functions defined over K^e and K^r. The reference shape functions are:

$$\begin{aligned} &\widehat{\boldsymbol{\xi}_1^r}(\hat{\mathbf{x}}) := (0,-1,1) \times (\hat{\mathbf{x}}) + (1,0,0), && \widehat{\boldsymbol{\xi}_2^r}(\hat{\mathbf{x}}) := (1,0,-1) \times (\hat{\mathbf{x}}) + (0,1,0), \\ &\widehat{\boldsymbol{\xi}_3^r}(\hat{\mathbf{x}}) := (-1,1,0) \times (\hat{\mathbf{x}}) + (0,0,1), && \widehat{\boldsymbol{\xi}_4^r}(\hat{\mathbf{x}}) := (0,0,1) \times (\hat{\mathbf{x}}), \\ &\widehat{\boldsymbol{\xi}_5^r}(\hat{\mathbf{x}}) := (1,0,0) \times (\hat{\mathbf{x}}), && \widehat{\boldsymbol{\xi}_6^r}(\hat{\mathbf{x}}) := (0,1,0) \times (\hat{\mathbf{x}}), \end{aligned} \tag{6}$$

where $\hat{\mathbf{x}} := (\widehat{x_1}, \widehat{x_2}, \widehat{x_3}) \in \overline{K^r}$ and $\overline{K^r}$ is the reference tetrahedron, see Fig. 1.

Now, we will state the element approximation property. To this end we introduce an interpolation operator $\boldsymbol{\pi}^e\colon\ [C^\infty(\overline{K^e})]^3 \mapsto \mathbf{P}^e$ such that

$$\sigma_i^e(\boldsymbol{\pi}^e(\mathbf{v})) = \sigma_i^e(\mathbf{v}), \quad i = 1, \ldots, 6,$$

holds for any $\mathbf{v} \in [C^\infty(\overline{K^e})]^3$. Further, we introduce a global interpolation operator $\boldsymbol{\pi}^h\colon\ [C^\infty(\overline{\Omega})]^3 \mapsto \mathbf{H}(\mathbf{curl}; \Omega)$ such that for any $\mathbf{v} \in [C^\infty(\overline{\Omega})]^3$ we have

$$\boldsymbol{\pi}^h(\mathbf{v})|_{K^e} := \boldsymbol{\pi}^e(\mathbf{v}|_{K^e}), \quad K^e \in \mathcal{T}^h.$$

The following definition and lemma are due to [22, p. 327].

Definition 1. A family $\mathcal{F} := \{\mathcal{T}^h \mid 0 < h \leqslant \overline{h}\}$ of decompositions (discretizations) of Ω into tetrahedra is said to be regular if there exists a constant $C_2 > 0$ such that for any $\mathcal{T}^h \in \mathcal{F}$ and any $K^e \in \mathcal{T}^h$ we have

$$\frac{h^e}{\varrho^e} \leqslant C_2, \tag{7}$$

where ϱ^e denotes the radius of the largest sphere inscribed in K^e.

Lemma 4. *Let $\mathcal{F}$ be a regular family of decompositions into tetrahedra in the sense of Definition* 1. *Then there exists a constant $C_3 > 0$ such that for any $\mathcal{T}^h \in \mathcal{F}$ we have*

$$\forall\, \mathbf{v} \in [C^\infty(\overline{\Omega})]^3\colon\ \|\mathbf{v} - \boldsymbol{\pi}^h(\mathbf{v})\|_{\mathbf{curl},\Omega} \leqslant C_3 h |\mathbf{v}|_{[H^2(\Omega)]^3}.$$

Proof. The assertion is a direct consequence of [22, Th. 2]. □

Lemma 5. *Let $\mathbf{v} \in [C_0^\infty(\Omega)]^3$ and let $\mathcal{F}$ be a regular family of decompositions. Then there exists a positive constant $C_4 \equiv C_4(\mathbf{v})$ such that for any $\mathcal{T}^h \in \mathcal{F}$ the following holds:*

$$\forall\, K^e \in \mathcal{T}^h\ \forall\, \mathbf{x} \equiv \boldsymbol{\mathcal{R}}^e(\hat{\mathbf{x}}) \in \overline{K^e}\colon\ \|\mathbf{curl}_{\mathbf{x}}(\boldsymbol{\pi}^e(\mathbf{v}|_{\overline{K^e}}))\| \leqslant C_4.$$

Proof. Let $\mathbf{v} \in [C_0^\infty(\Omega)]^3$ be an arbitrary function, $\mathcal{T}^h$ a regular discretization of Ω, and $K^e \in \mathcal{T}^h$ an element domain. The rotations of the reference shape functions, see (6), are constant over $\overline{K^r}$, e.g., $\mathbf{curl}_{\hat{\mathbf{x}}}(\widehat{\boldsymbol{\xi}}_1^r(\hat{\mathbf{x}})) = (0, -2, 2)$. Let us denote

$\sigma_i^e := \sigma_i^e(\mathbf{v}|_{\overline{K^e}})$ for $i = 1, 2, \ldots, 6$. Now, an application of the Stokes theorem yields

$$\mathbf{curl}_{\mathbf{x}}(\boldsymbol{\pi}^e(\mathbf{v}|_{\overline{K^e}}(\mathbf{x}))) = \frac{1}{\det(\mathbf{R}^e)} \sum_{i=1}^{6} \sigma_i^e(\mathbf{v}|_{\overline{K^e}}) \mathbf{R}^e \cdot \mathbf{curl}_{\hat{\mathbf{x}}}(\widehat{\boldsymbol{\xi}}_i^r(\hat{\mathbf{x}})) = \frac{2}{6\,\mathrm{meas}(K^e)}$$

$$\times \begin{pmatrix} (x_{2,1}^e - x_{1,1}^e)(\sigma_2^e - \sigma_3^e + \sigma_5^e) + (x_{3,1}^e - x_{1,1}^e)(\sigma_3^e - \sigma_1^e + \sigma_6^e) + (x_{4,1}^e - x_{1,1}^e)(\sigma_1^e - \sigma_2^e + \sigma_4^e) \\ (x_{2,2}^e - x_{1,2}^e)(\sigma_2^e - \sigma_3^e + \sigma_5^e) + (x_{3,2}^e - x_{1,2}^e)(\sigma_3^e - \sigma_1^e + \sigma_6^e) + (x_{4,2}^e - x_{1,2}^e)(\sigma_1^e - \sigma_2^e + \sigma_4^e) \\ (x_{2,3}^e - x_{1,3}^e)(\sigma_2^e - \sigma_3^e + \sigma_5^e) + (x_{3,3}^e - x_{1,3}^e)(\sigma_3^e - \sigma_1^e + \sigma_6^e) + (x_{4,3}^e - x_{1,3}^e)(\sigma_1^e - \sigma_2^e + \sigma_4^e) \end{pmatrix}$$

$$= \frac{-1}{3\,\mathrm{meas}(K^e)} \mathbf{R}^e \cdot \begin{pmatrix} \int_{f_2^e} \mathbf{curl}_{\mathbf{x}}(\mathbf{v}|_{\overline{K^e}}(\mathbf{x})) \cdot \mathbf{n}_2^e(\mathbf{x})\,\mathrm{dS} \\ \int_{f_3^e} \mathbf{curl}_{\mathbf{x}}(\mathbf{v}|_{\overline{K^e}}(\mathbf{x})) \cdot \mathbf{n}_3^e(\mathbf{x})\,\mathrm{dS} \\ \int_{f_4^e} \mathbf{curl}_{\mathbf{x}}(\mathbf{v}|_{\overline{K^e}}(\mathbf{x})) \cdot \mathbf{n}_4^e(\mathbf{x})\,\mathrm{dS} \end{pmatrix},$$

where f_2^e, f_3^e, f_4^e denote faces that are opposite to the nodes $\mathbf{x}_2^e$, $\mathbf{x}_3^e$, $\mathbf{x}_4^e$, respectively, and $\mathbf{n}_2^e$, $\mathbf{n}_3^e$, $\mathbf{n}_4^e$ are the outward normal vectors. From the regularity condition (7) it is obvious that $\mathrm{meas}(K^e) \geqslant \frac{4}{3}\pi(\varrho^e)^3 \geqslant \frac{4}{3}\pi(h^e/C_2)^3$. By estimating the integrals we arrive at

$$\|\mathbf{curl}_{\mathbf{x}}(\boldsymbol{\pi}^e(\mathbf{v}|_{\overline{K^e}}(\mathbf{x})))\| \leqslant \frac{3 \max_{\mathbf{x}\in\Omega} \|\mathbf{curl}_{\mathbf{x}}(\mathbf{v}(\mathbf{x}))\| (C_2)^3}{8\pi} =: C_4,$$

where we have considered $\|\mathbf{R}^e\| := \max_{i,j} |x_{i,j}^e - x_{1,j}^e|$. □

2.5.2. Discretized problem

Let Ω_0^h and Ω_1^h approximate the subdomains Ω_0 and Ω_1 so that

$$\forall K^e \in \mathcal{T}^h\colon\ K^e \subset \Omega_0^h \quad \text{or} \quad K^e \subset \Omega_1^h$$

and let $\mu^h(\mathbf{x})$ denote a discretization of the permeability function $\mu(\mathbf{x})$. The regularized bilinear form a_ε is approximated as follows:

$$a_\varepsilon^h(\mathbf{v}, \mathbf{u}) := \int_{\Omega_0^h} \frac{1}{\mu_0} \mathbf{curl}(\mathbf{v}) \cdot \mathbf{curl}(\mathbf{u})\,\mathrm{dx} + \int_{\Omega_1^h} \frac{1}{\mu_1} \mathbf{curl}(\mathbf{v}) \cdot \mathbf{curl}(\mathbf{u})\,\mathrm{dx} + \varepsilon \int_\Omega \mathbf{v} \cdot \mathbf{u}\,\mathrm{dx},$$

where $\mathbf{v}, \mathbf{u} \in \mathbf{H_0}(\mathbf{curl}; \Omega)$. The discretization of (W_ε) reads as follows:

$$(\mathrm{W}_\varepsilon^h) \qquad \begin{cases} \text{Find } \mathbf{u}_\varepsilon^h \in \mathbf{H_0}(\mathbf{curl}; \Omega)^h\colon \\ a_\varepsilon^h(\mathbf{v}^h, \mathbf{u}_\varepsilon^h) = f(\mathbf{v}^h) \quad \forall\, \mathbf{v}^h \in \mathbf{H_0}(\mathbf{curl}; \Omega)^h. \end{cases}$$

The existence of a unique solution can be proven similarly as in Lemma 2.

2.5.3. The convergence property

Lemma 6. *Let Assumption* 1 *hold and let us consider a regular family* $\mathcal{F}$ *of decompositions* $\mathcal{T}^h$. *Assume that*

$$|\mu^h(\mathbf{x}) - \mu(\mathbf{x})| \to 0 \quad \text{a.e. in } \Omega \text{ as } h \to 0_+. \tag{8}$$

Then for each $\varepsilon > 0$ *and* $h > 0$ *we have*

$$\mathbf{u}_\varepsilon^h \to \mathbf{u}_\varepsilon \quad \text{in } \mathbf{H_0(curl;}\Omega) \text{ as } h \to 0_+.$$

Proof. Let $\varepsilon > 0$ be arbitrary. The proof is based on the following first Strang's lemma, cf. [3]: There exists $C(\varepsilon) > 0$ such that for each $\mathbf{v}^h \in \mathbf{H_0(curl;}\Omega)^h$ we have

$$\|\mathbf{u}_\varepsilon - \mathbf{u}_\varepsilon^h\|_{\mathbf{curl},\Omega} \leqslant C(\varepsilon)\left\{\|\mathbf{u}_\varepsilon^h - \mathbf{v}^h\|_{\mathbf{curl},\Omega} + \frac{|a_\varepsilon(\mathbf{v}^h, \mathbf{u}_\varepsilon^h - \mathbf{v}^h) - a_\varepsilon^h(\mathbf{v}^h, \mathbf{u}_\varepsilon^h - \mathbf{v}^h)|}{\|\mathbf{u}_\varepsilon^h - \mathbf{v}^h\|_{\mathbf{curl},\Omega}}\right\}. \tag{9}$$

Now, the idea of the proof is like in [14, Th. 4.16], originally in [5]. Let $\tau > 0$ be arbitrary. By virtue of (2) there exists $\widetilde{\mathbf{u}}_\varepsilon \in [C_0^\infty(\Omega)]^3$ such that

$$\|\mathbf{u}_\varepsilon - \widetilde{\mathbf{u}}_\varepsilon\|_{\mathbf{curl},\Omega} \leqslant \frac{\tau}{4C(\varepsilon)}. \tag{10}$$

In the estimate (9) we choose $\mathbf{v}^h := \boldsymbol{\pi}^h(\widetilde{\mathbf{u}}_\varepsilon)$.

The first term on the right-hand side of (9) can be estimated as follows:

$$\begin{aligned}\|\mathbf{u}_\varepsilon - \mathbf{v}^h\|_{\mathbf{curl},\Omega} &= \|\mathbf{u}_\varepsilon - \widetilde{\mathbf{u}}_\varepsilon + \widetilde{\mathbf{u}}_\varepsilon - \mathbf{v}^h\|_{\mathbf{curl},\Omega} \\ &\leqslant \frac{\tau}{4C(\varepsilon)} + \|\widetilde{\mathbf{u}}_\varepsilon - \boldsymbol{\pi}^h(\widetilde{\mathbf{u}}_\varepsilon)\|_{\mathbf{curl},\Omega} \leqslant \frac{\tau}{4C(\varepsilon)} + C_3 h|\widetilde{\mathbf{u}}_\varepsilon|_{[H^2(\Omega)]^3},\end{aligned} \tag{11}$$

where we have used the triangle inequality, (10), and Lemma 4. The numerator of the second term on the right-hand side of (9) is

$$\begin{aligned}&|a_\varepsilon(\mathbf{v}^h, \mathbf{u}_\varepsilon^h - \mathbf{v}^h) - a_\varepsilon^h(\mathbf{v}^h, \mathbf{u}_\varepsilon^h - \mathbf{v}^h)| \\ &\quad = \left|\int_\Omega \mathbf{curl}(\mathbf{u}_\varepsilon^h - \mathbf{v}^h)\Big(\frac{1}{\mu} - \frac{1}{\mu^h}\Big)\mathbf{curl}(\mathbf{v}^h)\,\mathrm{d}\mathbf{x}\right| \\ &\quad \leqslant \|\mathbf{u}_\varepsilon^h - \mathbf{v}^h\|_{\mathbf{curl},\Omega}\sqrt{\int_\Omega \Big|\frac{1}{\mu} - \frac{1}{\mu^h}\Big|^2 \|\mathbf{curl}(\mathbf{v}^h)\|^2\,\mathrm{d}\mathbf{x}},\end{aligned} \tag{12}$$

where the Hölder inequality has been used. Now, by Lemma 5 there exists $C_4 > 0$ such that for any h, $0 < h \leqslant \overline{h}$, and for each $\mathbf{x} \in \overline{K^e} \subset \overline{\Omega}$ we have

$$\Big|\frac{1}{\mu(\mathbf{x})} - \frac{1}{\mu^h(\mathbf{x})}\Big|\|\mathbf{curl}(\mathbf{v}^h(\mathbf{x}))\| \leqslant \Big(\frac{1}{\mu_0} - \frac{1}{\mu_1}\Big)C_4(\widetilde{\mathbf{u}}_\varepsilon),$$

where we have also used (1). Then due to (8) and the Lebesgue dominated convergence theorem, cf. [21],

$$\int_\Omega \left|\frac{1}{\mu} - \frac{1}{\mu^h}\right|^2 \|\mathbf{curl}(\mathbf{v}^h)\|^2 \,\mathrm{d}\mathbf{x} \to 0 \quad \text{as } h \to 0_+. \tag{13}$$

Finally, dividing the inequality (12) by $\|\mathbf{u}_\varepsilon^h - \mathbf{v}^h\|_{\mathbf{curl},\Omega}$ and combining that with (9), (11), and (13) completes the proof. □

3. Optimal shape design

3.1. Admissible shapes

Let α stand for a shape which is a continuous function over a rectangle $\omega \subset \mathbb{R}^2$. We assume that there exists a common Lipschitz constant $C_5 > 0$ and box constraints $\alpha_\mathrm{l}, \alpha_\mathrm{u} \in \mathbb{R}$. Then the set of admissible shapes is

$$\mathcal{U} := \{\alpha \in C(\overline{\omega}) \mid \forall\, \mathbf{x}, \mathbf{y} \in \overline{\omega}\colon\ |\alpha(\mathbf{x}) - \alpha(\mathbf{y})| \leqslant C_5\|\mathbf{x} - \mathbf{y}\| \quad \text{and} \quad \alpha_\mathrm{l} \leqslant \alpha(\mathbf{x}) \leqslant \alpha_\mathrm{u}\},$$

equipped with the uniform convergence $\alpha_n \to \alpha$ in $\mathcal{U}$, i.e., $\alpha_n \rightrightarrows \alpha$ as $n \to \infty$.

Lemma 7. *$\mathcal{U}$ is compact.*

Proof. It follows from Theorem of Ascoli and Arzelà, cf. [11, p. 2]. □

In Section 4 we will deal with an application where in the end we will be looking for smooth shapes, e.g., Bézier curves or patches, cf. [6], rather than for continuous ones. To this end, being inspired by [4], we introduce a parameterization, i.e., a nonempty compact set of design parameters $\Upsilon \subset \mathbb{R}^{n_\Upsilon}$, $n_\Upsilon \in \mathbb{N}$, and a continuous nonsurjective mapping

$$F\colon\ \Upsilon \mapsto \mathcal{U}. \tag{14}$$

Finally, without loss of generality we assume that the shape α controls the following decomposition of Ω into the subdomains $\Omega_0(\alpha)$ and $\Omega_1(\alpha)$:

$$\overline{\Omega} = \overline{\Omega_0(\alpha)} \cup \overline{\Omega_1(\alpha)}, \quad \Omega_0(\alpha) \cap \Omega_1(\alpha) = \emptyset \tag{15}$$
$$\text{such that } \operatorname{graph}(\alpha) \subset \partial\Omega_0(\alpha) \cap \partial\Omega_1(\alpha) \text{ and } \operatorname{meas}(\Omega_0(\alpha)), \operatorname{meas}(\Omega_1(\alpha)) > 0,$$

an example of which is depicted in Fig. 2. Recall that the graph is defined by

$$\operatorname{graph}(\alpha) := \{(x_1, x_2, y) \in \mathbb{R}^3 \mid \mathbf{x} := (x_1, x_2) \in \overline{\omega} \quad \text{and} \quad y = \alpha(\mathbf{x})\}.$$

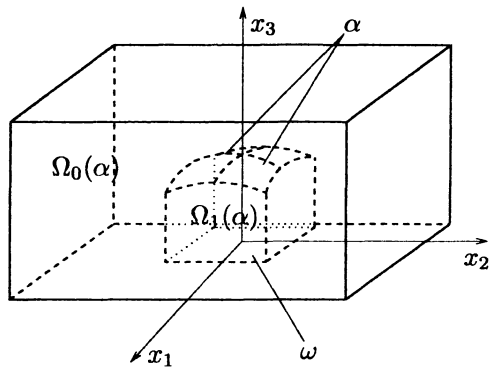

Figure 2. Decomposition of Ω.

3.2. Multistate problem

Only the piecewise constant permeability μ depends by (15) on α, thus,

$$a_\alpha(\mathbf{v},\mathbf{u}) := \int_{\Omega_0(\alpha)} \frac{1}{\mu_0}\mathbf{curl}(\mathbf{v})\cdot\mathbf{curl}(\mathbf{u})\,\mathrm{d}\mathbf{x} + \int_{\Omega_1(\alpha)} \frac{1}{\mu_1}\mathbf{curl}(\mathbf{v})\cdot\mathbf{curl}(\mathbf{u})\,\mathrm{d}\mathbf{x}.$$

Moreover, we consider n_{v} state problems that only differ by the current $\mathbf{J}^v$,

$$f^v(\mathbf{v}) := \int_\Omega \mathbf{J}^v\cdot\mathbf{v}\,\mathrm{d}\mathbf{x}, \quad v = 1,\dots,n_{\mathrm{v}},$$

so that (3) still holds. For any $\alpha\in\mathcal{U}$ and $v\in 1,\dots,n_{\mathrm{v}}$ we consider the following state problem, which is uniquely solvable:

$$(\mathrm{W}^v(\alpha)) \qquad \begin{cases} \text{Find } \mathbf{u}^v(\alpha)\in\mathbf{H}_{0,\perp}(\mathbf{curl};\Omega): \\ a_\alpha(\mathbf{v},\mathbf{u}^v(\alpha)) = f^v(\mathbf{v}) \quad \forall\,\mathbf{v}\in\mathbf{H}_{0,\perp}(\mathbf{curl};\Omega) \end{cases}$$

Lemma 8. *For each v the mapping $\mathbf{u}^v\colon \mathcal{U}\mapsto\mathbf{H}_{0,\perp}(\mathbf{curl};\Omega)$ is continuous.*

Proof. Let $v = 1,\dots,n_{\mathrm{v}}$ be arbitrary and let $\{\alpha_n\}\subset\mathcal{U}$ be a sequence such that $\alpha_n \rightrightarrows \alpha$, where $\alpha\in\mathcal{U}$. For simplicity, we set $\mathbf{u} := \mathbf{u}^v(\alpha)$ and $\mathbf{u}_n := \mathbf{u}^v(\alpha_n)$. We observe that (4) holds independently of α. Thus, by $(\mathrm{W}^v(\alpha_n))$ and $(\mathrm{W}^v(\alpha))$,

$$\begin{aligned} (16) \qquad \|\mathbf{u}_n-\mathbf{u}\|^2_{\mathbf{curl},\Omega} &\leqslant \mu_1 C_1^2 a_{\alpha_n}(\mathbf{u}_n-\mathbf{u},\mathbf{u}_n-\mathbf{u}) \\ &= \mu_1 C_1^2 (f^v(\mathbf{u}_n-\mathbf{u}) - a_{\alpha_n}(\mathbf{u}_n-\mathbf{u},\mathbf{u})) \\ &= \mu_1 C_1^2 (a_\alpha(\mathbf{u}_n-\mathbf{u},\mathbf{u}) - a_{\alpha_n}(\mathbf{u}_n-\mathbf{u},\mathbf{u})). \end{aligned}$$

Further, we denote the characteristic functions of the sets $\Omega_0(\alpha)$ and $\Omega_1(\alpha)$ by $\chi_0(\mathbf{x},\alpha)$ and $\chi_1(\mathbf{x},\alpha)$, respectively. Since $\alpha_n \rightrightarrows \alpha$, we have

$$(17) \qquad \chi_0(\mathbf{x},\alpha_n)\to\chi_0(\mathbf{x},\alpha) \text{ and } \chi_1(\mathbf{x},\alpha_n)\to\chi_1(\mathbf{x},\alpha) \text{ a.e. in } \Omega \text{ as } n\to\infty.$$

Now, using the Cauchy-Schwarz inequality in $[L^2(\Omega)]^3$ yields

$$
\begin{aligned}
(18)\quad & |a_\alpha(\mathbf{u}_n - \mathbf{u}, \mathbf{u}) - a_{\alpha_n}(\mathbf{u}_n - \mathbf{u}, \mathbf{u})| \\
&= \frac{1}{\mu_0}\int_\Omega \{(\chi_0(\mathbf{x},\alpha) - \chi_0(\mathbf{x},\alpha_n))\mathbf{curl}(\mathbf{u})\}\cdot\mathbf{curl}(\mathbf{u}_n - \mathbf{u})\,\mathrm{d}\mathbf{x} \\
&\quad + \frac{1}{\mu_1}\int_\Omega \{(\chi_1(\mathbf{x},\alpha) - \chi_1(\mathbf{x},\alpha_n))\mathbf{curl}(\mathbf{u})\}\cdot\mathbf{curl}(\mathbf{u}_n - \mathbf{u})\,\mathrm{d}\mathbf{x} \\
&\leqslant \frac{1}{\mu_0}(\|(\chi_0(\mathbf{x},\alpha) - \chi_0(\mathbf{x},\alpha_n))\mathbf{curl}(\mathbf{u})\|_{[L^2(\Omega)]^3} \\
&\quad + \|(\chi_1(\mathbf{x},\alpha) - \chi_1(\mathbf{x},\alpha_n))\mathbf{curl}(\mathbf{u})\|_{[L^2(\Omega)]^3})\cdot\|\mathbf{curl}(\mathbf{u}_n - \mathbf{u})\|_{[L^2(\Omega)]^3}.
\end{aligned}
$$

From (17), for $i = 0, 1$, $|\chi_i(\mathbf{x};\alpha) - \chi_i(\mathbf{x};\alpha_n)|^2\|\mathbf{curl}(\mathbf{u}(\mathbf{x}))\|^2 \to 0$ a.e. Ω as $n \to \infty$. Now, by the Lebesgue dominated convergence theorem, cf. [21, p. 26], the right-hand side of (18) tends to zero. Together with (16) this completes the proof. □

3.3. Shape optimization problem

Let $\mathcal{I}\colon \mathcal{U} \times [\mathbf{H_0(curl};\Omega)]^{n_v} \mapsto \mathbb{R}$ be a continuous functional. Using $(\mathrm{W}^v(\alpha))$, we define the cost functional $\mathcal{J}\colon \mathcal{U} \mapsto \mathbb{R}$ by $\mathcal{J}(\alpha) := \mathcal{I}(\alpha, \mathbf{u}^1(\alpha), \ldots, \mathbf{u}^{n_v}(\alpha))$. The continuous optimization problem is then formulated as follows:

$$
(\mathrm{P})\qquad \begin{cases} \text{Find } \alpha^* \in \mathcal{U}\colon \\ \mathcal{J}(\alpha^*) \leqslant \mathcal{J}(\alpha) \quad \forall\, \alpha \in \mathcal{U}. \end{cases}
$$

Theorem 1. *There exists $\alpha^* \in \mathcal{U}$ which is a solution to* (P).

Proof. By Lemma 7, $\mathcal{U}$ is a compact subset of the normed linear space $C(\overline{\omega})$. Using the continuity of $\mathcal{I}$ and Lemma 8 we obtain the continuity of $\mathcal{J}$ on $\mathcal{U}$. Now the assertion follows from a classical theorem, cf. [11, Th. 1.3]. □

Moreover, we use (14) to define the cost functional $\widetilde{\mathcal{J}}\colon \Upsilon \mapsto \mathbb{R}$ by $\widetilde{\mathcal{J}}(\mathbf{p}) := \mathcal{J}(F(\mathbf{p}))$. Then, by the compactness of Υ, the continuity of F on Υ, and Theorem 1, there exists a solution to the finite-dimensional optimization problem

$$
(\widetilde{\mathrm{P}})\qquad \begin{cases} \text{Find } \mathbf{p}^* \in \Upsilon\colon \\ \widetilde{\mathcal{J}}(\mathbf{p}^*) \leqslant \widetilde{\mathcal{J}}(\mathbf{p}) \;\; \forall\, \mathbf{p} \in \Upsilon. \end{cases}
$$

3.4. Regularization of the bilinear form

Similarly to Section 2.4, the regularized weak formulation reads as follows:

$$
(\mathrm{W}^v_\varepsilon(\alpha))\qquad \begin{cases} \text{Find } \mathbf{u}^v_\varepsilon(\alpha) \in \mathbf{H_0(curl};\Omega)\colon \\ a_{\varepsilon,\alpha}(\mathbf{v}, \mathbf{u}^v_\varepsilon(\alpha)) = f^v(\mathbf{v}) \quad \forall\, \mathbf{v} \in \mathbf{H_0(curl};\Omega), \end{cases}
$$

where $a_{\varepsilon,\alpha}(\mathbf{v},\mathbf{u}) := a_\alpha(\mathbf{v},\mathbf{u}) + \varepsilon \int_\Omega \mathbf{v}\cdot\mathbf{u}\,\mathrm{d}\mathbf{x}$. The corresponding shape optimization problem reads

$$(\mathrm{P}_\varepsilon) \qquad \begin{cases} \text{Find } \alpha_\varepsilon{}^* \in \mathcal{U}: \\ \mathcal{J}_\varepsilon(\alpha_\varepsilon{}^*) \leqslant \mathcal{J}_\varepsilon(\alpha) \quad \forall\, \alpha \in \mathcal{U}, \end{cases}$$

where $\mathcal{J}_\varepsilon(\alpha) := \mathcal{I}(\alpha, \mathbf{u}_\varepsilon^1(\alpha), \ldots, \mathbf{u}_\varepsilon^{n_\mathrm{v}}(\alpha))$. The existence of an optimal solution to (P_ε) can be proven as in Theorem 1.

Theorem 2. *Let $\{\varepsilon_n\}_{n=1}^\infty \subset \mathbb{R}$ be a sequence of positive regularization parameters such that $\varepsilon_n \to 0_+$ as $n \to \infty$, and let $\alpha_{\varepsilon_n}{}^*$ be the corresponding solutions to $(\mathrm{P}_{\varepsilon_n})$. Then there exist a subsequence $\{\varepsilon_{n_k}\}_{k=1}^\infty \subset \{\varepsilon_n\}_{n=1}^\infty$ and a shape $\alpha^* \in \mathcal{U}$ such that*

$$\alpha_{\varepsilon_{n_k}}{}^* \to \alpha^* \quad \text{in } \mathcal{U} \text{ as } k \to \infty$$

holds and, moreover, α^* is a solution to (P).

Proof. Here we make use of Lemma 3, see [11] or [17, p. 73]. □

3.5. Finite element approximation

Let $h > 0$ be a discretization parameter as in Section 2.5. Referring to Fig. 3 we will introduce a finite-dimensional approximation of $\mathcal{U}$. Let $\mathcal{T}_\omega^h := \{\omega_1^h, \ldots, \omega_{n_\omega^h}^h\}$, where $n_\omega^h \in \mathbb{N}$, be a triangulation of a rectangular domain ω. Let $P^1(\mathcal{T}_\omega^h)$ denote the space of continuous functions that are linear over each $\overline{\omega_i^h}$. Then the discretized set of admissible shapes is

$$\mathcal{U}^h := \{\alpha^h \in P^1(\mathcal{T}_\omega^h) \mid \forall\, \mathbf{x},\mathbf{y} \in \overline{\omega}\colon\ |\alpha^h(\mathbf{x}) - \alpha^h(\mathbf{y})| \leqslant C_5\|\mathbf{x}-\mathbf{y}\| \text{ and } \alpha_\mathrm{l} \leqslant \alpha^h(\mathbf{x}) \leqslant \alpha_\mathrm{u}\}.$$

The set $\mathcal{U}^h$ is clearly finite-dimensional and closed, and thus, compact. Let $\pi_\omega^h\colon \mathcal{U} \mapsto P^1(\mathcal{T}_\omega^h)$ interpolate shapes at the nodes of $\mathcal{T}_\omega^h$. Then, as in [1],

$$\forall\, \alpha \in \mathcal{U}\colon\ \pi_\omega^h(\alpha) \rightrightarrows \alpha \text{ as } h \to 0_+. \tag{19}$$

Again, given a discretized shape α^h, we consider the decomposition of Ω into $\Omega_0(\alpha^h)$ and $\Omega_1(\alpha^h)$, an example of which is depicted in Fig. 3. We provide a discretization $\mathcal{T}^h(\alpha^h) := \{K^{e_1}(\alpha^h), \ldots, K^{e_{n_\Omega}}(\alpha^h)\}$ of Ω such that

$$\forall\, K^{e_i}(\alpha^h) \in \mathcal{T}^h(\alpha^h)\colon\ K^{e_i}(\alpha^h) \subset \Omega_0(\alpha^h) \text{ or } K^{e_i}(\alpha^h) \subset \Omega_1(\alpha^h).$$

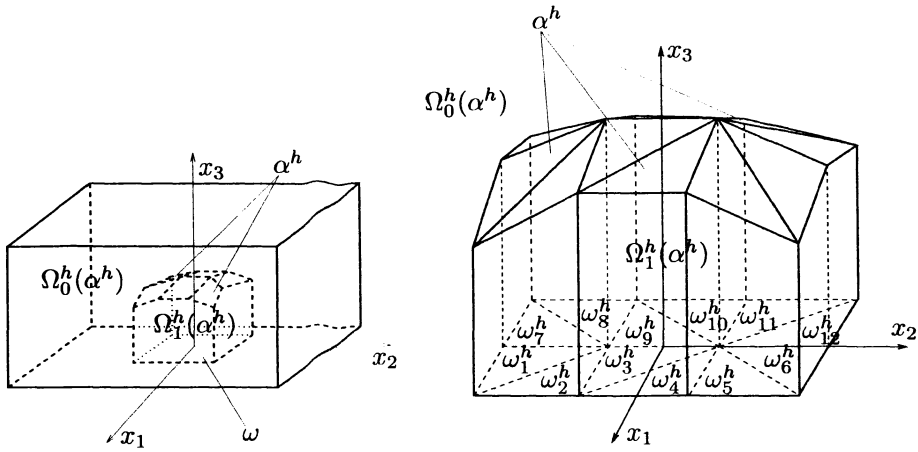

Figure 3. Decomposition of Ω^h.

Assumption 2. We assume that for any $h > 0$ fixed ($h \leqslant \overline{h}$) the connectivity of the discretization grid $\mathcal{T}^h(\alpha^h)$ is independent of α^h, we further assume that the corners $\mathbf{x}_1^{e_i}(\alpha^h), \ldots, \mathbf{x}_4^{e_i}(\alpha^h)$ of $K^{e_i}(\alpha^h)$ form a tetrahedron and they depend continuously on α^h.

The regularized and discretized multistate problem is

$$(\mathrm{W}_\varepsilon^{v,h}(\alpha^h)) \qquad \begin{cases} \text{Find } \mathbf{u}_\varepsilon^{v,h}(\alpha^h) \in \mathbf{H_0(curl;}\Omega;\alpha^h)^h: \\ a_{\varepsilon,\alpha^h}(\mathbf{v}^h, \mathbf{u}_\varepsilon^{v,h}(\alpha^h)) = f^v(\mathbf{v}^h) \quad \forall\, \mathbf{v}^h \in \mathbf{H_0(curl;}\Omega;\alpha^h)^h. \end{cases}$$

The existence of a unique solution to $(\mathrm{W}_\varepsilon^{v,h}(\alpha^h))$ is easy to prove.

Lemma 9. *For each $v = 1, \ldots, n_\mathrm{v}$, $\varepsilon > 0$ and $h > 0$ ($h \leqslant \overline{h}$) the mapping $\mathbf{u}_\varepsilon^{v,h}$: $\mathcal{U}^h \mapsto \mathbf{H_0(curl;}\Omega)$ is continuous.*

Proof. Now we cannot use the same technique as in the proof of Lemma 8, since the settings $(\mathrm{W}_\varepsilon^{v,h}(\alpha^h))$ differ from $\alpha^h \in \mathcal{U}^h$. Therefore, the estimate (16) cannot be established. Instead, we have to exploit the algebraic structure of the mapping $\mathbf{u}_\varepsilon^{v,h}$. The proof is given in [17, p. 77]. □

Lemma 10. *Let $\varepsilon > 0$, $\{h_n\}_{n=1}^\infty \subset \mathbb{R}$, $0 < h_n \leqslant \overline{h}$, be such that $h_n \to 0_+$ as $n \to \infty$, and let $\alpha \in \mathcal{U}$, $\{\alpha^{h_n}\}_{n=1}^\infty \subset \mathcal{U}$, $\alpha^{h_n} \in \mathcal{U}^{h_n}$, be such that $\alpha^{h_n} \to \alpha$ in $\mathcal{U}$ as $n \to \infty$. Then for each $v = 1, \ldots, n_\mathrm{v}$ we have*

$$\mathbf{u}_\varepsilon^{v,h_n}(\alpha^{h_n}) \to \mathbf{u}_\varepsilon^v(\alpha) \text{ in } \mathbf{H_0(curl;}\Omega) \text{ as } n \to \infty,$$

where $\mathbf{u}_\varepsilon^{v,h_n}(\alpha^{h_n})$ is the solution to $(\mathrm{W}_\varepsilon^{v,h_n}(\alpha^{h_n}))$ and $\mathbf{u}_\varepsilon^v(\alpha)$ solves $(\mathrm{W}_\varepsilon^v(\alpha))$.

P r o o f. It is enough to prove that the assumption (8) is fulfilled and the rest follows from Lemma 6. We specify $\mu(\mathbf{x}) \equiv \mu_\alpha(\mathbf{x})$ and $\mu^{h_n}(\mathbf{x}) \equiv \mu_{\alpha^{h_n}}(\mathbf{x})$, where

$$\mu_\alpha(\mathbf{x}) := \begin{cases} \mu_0, & \mathbf{x} \in \Omega_0(\alpha), \\ \mu_1, & \mathbf{x} \in \Omega_1(\alpha), \end{cases} \qquad \alpha \in \mathcal{U}.$$

Let us take an arbitrary point $\mathbf{x} \in \Omega_0(\alpha) \cup \Omega_1(\alpha)$. We suppose that $\mathbf{x} \in \Omega_0(\alpha)$, i.e., $\mu_\alpha(\mathbf{x}) = \mu_0$ while the other case is an analogue. Since $\alpha^{h_n} \rightrightarrows \alpha$ for $n \to \infty$, there exists $n_0 \in \mathbb{N}$ such that $\mathbf{x} \in \Omega_0(\alpha^{h_n})$ for all $n \geqslant n_0$, thus, $\mu_{\alpha^{h_n}}(\mathbf{x}) = \mu_\alpha(\mathbf{x}) = \mu_0$ and the proof is complete. □

The relevant setting of the shape optimization problem reads

$$(\mathrm{P}_\varepsilon^h) \qquad \begin{cases} \text{Find } \alpha_\varepsilon^{h\,*} \in \mathcal{U}^h: \\ \mathcal{J}_\varepsilon^h(\alpha_\varepsilon^{h\,*}) \leqslant \mathcal{J}_\varepsilon^h(\alpha^h) \quad \forall\, \alpha^h \in \mathcal{U}^h, \end{cases}$$

where $\mathcal{J}_\varepsilon^h(\alpha^h) := \mathcal{I}(\alpha^h, \mathbf{u}_\varepsilon^{1,h}(\alpha^h), \ldots, \mathbf{u}_\varepsilon^{n_\mathrm{v},h}(\alpha^h))$. The existence theorem holds.

Theorem 3. *Let $\varepsilon > 0$, let $\{h_n\}_{n=1}^\infty \subset \mathbb{R}$, $0 < h_n \leqslant \overline{h}$, be such that $h_n \to 0_+$ as $n \to \infty$, and let $\alpha_\varepsilon^{h_n\,*} \in \mathcal{U}^{h_n}$ denote the corresponding solutions to $(\mathrm{P}_\varepsilon^{h_n})$. Then there exist a subsequence $\{h_{n_k}\}_{k=1}^\infty \subset \{h_n\}_{n=1}^\infty$ and a shape $\alpha_\varepsilon{}^* \in \mathcal{U}$ such that*

$$\alpha_\varepsilon^{h_{n_k}\,*} \to \alpha_\varepsilon{}^* \text{ in } \mathcal{U} \quad \text{as } k \to \infty$$

holds and, moreover, $\alpha_\varepsilon{}^*$ is a solution to the problem (P_ε).

P r o o f. By Lemma 7, there exist a subsequence of optimized shapes $\{\alpha_\varepsilon^{h_{n_k}\,*}\}_{k=1}^\infty \subset \{\alpha_\varepsilon^{h_n\,*}\}_{n=1}^\infty$ and a shape $\alpha_\varepsilon{}^* \in \mathcal{U}$ such that

$$\alpha_\varepsilon^{h_{n_k}\,*} \to \alpha_\varepsilon{}^* \text{ in } \mathcal{U} \quad \text{as } k \to \infty. \tag{20}$$

Let $\alpha \in \mathcal{U}$ be an arbitrary shape. For any $k \in \mathbb{N}$, by the definition of $(\mathrm{P}_\varepsilon^{h_{n_k}})$ and since $\pi_\omega^{h_{n_k}}(\alpha) \in \mathcal{U}^{h_{n_k}}$, we have

$$\mathcal{J}_\varepsilon^{h_{n_k}}(\alpha_\varepsilon^{h_{n_k}\,*}) \leqslant \mathcal{J}_\varepsilon^{h_{n_k}}(\pi_\omega^{h_{n_k}}(\alpha)). \tag{21}$$

Using (19) or (20), Lemma (10), and the continuity of $\mathcal{I}$, the right- or left-hand side of (21) respectively converges to $\mathcal{J}_\varepsilon(\alpha)$ or $\mathcal{J}_\varepsilon(\alpha_\varepsilon{}^*)$ as $k \to \infty$. □

Finally, we introduce the regularized and discretized cost functional $\widetilde{\mathcal{J}}_\varepsilon^h\colon \Upsilon \mapsto \mathbb{R}$ by $\widetilde{\mathcal{J}}_\varepsilon^h(\mathbf{p}) := \mathcal{J}_\varepsilon^h(\pi_\omega^h(F(\mathbf{p})))$. The related optimization problem is

$$(\widetilde{\mathrm{P}}_\varepsilon^h) \qquad \begin{cases} \text{Find } \mathbf{p}_\varepsilon^{h\,*} \in \Upsilon\colon \\ \widetilde{\mathcal{J}}_\varepsilon^h(\mathbf{p}_\varepsilon^{h\,*}) \leqslant \widetilde{\mathcal{J}}_\varepsilon^h(\mathbf{p}) \quad \forall\, \mathbf{p} \in \Upsilon. \end{cases}$$

Remark 1. In cases of complex geometries, as that in Section 4, Assumption 2 is a serious bottleneck of this discretization approach. For small discretization parameters and large changes in the design we cannot guarantee that the perturbed elements still satisfy the regularity condition. They might be even flipped. In this case, we have to re-mesh the geometry and solve the optimization problem again, but now on a grid of different topology. Then certainly the cost functional is not continuous any more and the just introduced convergence theory cannot be applied. Nevertheless, in literature this approach is still the most frequently used one as far as a finite element discretization is concerned. In practice, after we get an optimized shape we should compare the value of a very fine discretized cost functional for the optimized design with the value of the initial one. If we can see a progress then the optimization surely did a good job. Some solutions to this inconsistency between the theory and practice are discussed in Conclusions.

3.6. Sensitivity analysis

We will solve $(\widetilde{\mathrm{P}}_\varepsilon^h)$ by sequential quadratic programming with an updating formula of the Hessian matrix. To this end we have to provide the gradient of the cost functional $\widetilde{\mathcal{J}}_\varepsilon^h$ with respect to the design parameters $\mathbf{p}$. Let us note that the gradient of the constraint functional $\boldsymbol{v}^h\colon \mathbb{R}^{n_\Upsilon} \mapsto \mathbb{R}^{n_{\boldsymbol{v}^h}}$, where $n_{\boldsymbol{v}^h} \in \mathbb{N}$, which is defined so that

$$\Upsilon = \{\mathbf{p} \in \mathbb{R}^{n_\Upsilon} \mid \boldsymbol{v}^h(\mathbf{p}) \leqslant \mathbf{0}\}$$

can be easily calculated by hand. The evaluation of the cost functional proceeds as follows:

$$\mathbf{p} \xrightarrow{\pi_\omega^h \circ F} \boldsymbol{\alpha}^h \xrightarrow{\boldsymbol{K}^h \cdot \triangle \mathbf{x}^h = \boldsymbol{b}^h(\boldsymbol{\alpha}^h)} \mathbf{x}^h \xrightarrow{\text{FEM}} \boldsymbol{A}_\varepsilon^n, \boldsymbol{f}^{v,n} \xrightarrow{\boldsymbol{A}_\varepsilon^n \cdot \boldsymbol{u}_\varepsilon^{v,n} = \boldsymbol{f}^{v,n}} \xrightarrow{\boldsymbol{A}_\varepsilon^n \cdot \boldsymbol{u}_\varepsilon^{v,n} = \boldsymbol{f}^{v,n}} \boldsymbol{u}_\varepsilon^{v,n} \xrightarrow{\mathcal{I}^h(\boldsymbol{\alpha}^h, \mathbf{x}^h, \boldsymbol{u}_\varepsilon^{1,n_\Omega}, \ldots, \boldsymbol{u}_\varepsilon^{n_V, n_\Omega})} \widetilde{\mathcal{J}}_\varepsilon^h(\mathbf{p}),$$

where the shape-to-mesh mapping

$$\boldsymbol{K}^h \cdot \triangle \mathbf{x}^h(\boldsymbol{\alpha}^h) = \boldsymbol{b}^h(\boldsymbol{\alpha}^h)$$

maps the shape nodal coordinates $\boldsymbol{\alpha}^h$ onto the remaining nodal coordinates $\mathbf{x}^h$ in the grid. It is based on solving an auxiliary discretized 3d linear elasticity problem

in terms of grid displacements $\triangle \mathbf{x}^h(\boldsymbol{\alpha}^h)$ with a nonhomogeneous Dirichlet boundary condition that corresponds to the given shape displacements $\boldsymbol{\alpha}^h$, and with zero displacements on $\partial\Omega$ and on the boundaries of the subdomains with nonzero current density $\mathbf{J}^v$. Here, $\boldsymbol{K}^h \equiv \boldsymbol{K}^h(\mathbf{x}_0^h)$ is a nonsingular stiffness matrix assembled on the initial grid $\mathbf{x}_0^h$ and $\boldsymbol{b}^h(\boldsymbol{\alpha}^h)$ is the right-hand side vector linearly dependent on $\boldsymbol{\alpha}^h$. The resulting mesh is then calculated by

$$\mathbf{x}^h(\boldsymbol{\alpha}^h) := \mathbf{x}_0^h + \triangle \mathbf{x}^h(\boldsymbol{\alpha}^h) + \boldsymbol{M}^h(\boldsymbol{\alpha}^h),$$

where $\boldsymbol{M}^h\colon\ \mathbb{R}^{3n_{\boldsymbol{\alpha}^h}} \mapsto \mathbb{R}^{3n_{\mathbf{x}^h}}$ identically maps the nodal coordinates of the shape α^h onto the corresponding coordinates in the grid vector $\mathbf{x}^h$.

We can guarantee the smoothness of $\widetilde{\mathcal{J}}_\varepsilon^h$ via the smoothness of its individual submappings, see [17, p. 87]. Then we are justified to use a Newton-like algorithm.

Concerning the gradient of the cost functional, we use the chain rule to differentiate the cost functional. Then, we apply the adjoint method which evaluates the resulting expression from right to left. Since there is no state dependent constraint, the adjoint method involves only n_{v} additional solutions of the state systems $\boldsymbol{A}_\varepsilon^n$ with the right-hand sides $\mathbf{grad}_{\boldsymbol{u}_\varepsilon^{v,n}}(\mathcal{I}^h)$. Moreover, we have to assemble the derivatives of the element matrices with respect to the grid nodal displacements. They mainly involve derivatives of the matrix $\mathbf{R}^e$ and of its determinant, see (5). The computational effort is comparable to the assembling of the system matrix. The multistate problem sensitivity is then aggregated for each state as follows:

$$\sum_{v=1}^{n_{\mathrm{v}}} \left[-\frac{\partial \boldsymbol{A}_\varepsilon^n}{\partial [\mathbf{x}_1^h]_1} \cdot \boldsymbol{u}_\varepsilon^{v,n}, \ldots, -\frac{\partial \boldsymbol{A}_\varepsilon^n}{\partial [\mathbf{x}_{n_{\mathbf{x}^h}}^h]_3} \cdot \boldsymbol{u}_\varepsilon^{v,n} \right]^T \cdot (\boldsymbol{A}_\varepsilon^n)^{-1} \cdot \mathbf{grad}_{\boldsymbol{u}_\varepsilon^{v,n}}(\mathcal{I}^h).$$

In [17], [19] we develop an efficient object-oriented implementation for shape sensitivity analysis governed by various linear elliptic 2nd-order partial differential equations, where the only part which has always to be recoded by a user is the formula for $\mathcal{I}^h$.

4. An application

4.1. Physical problem

We consider an electromagnet of the Maltese Cross (MC) geometry, as depicted in Fig. 4. It consists of a ferromagnetic yoke and 4 poles completed with coils which are pumped with direct electric currents.

The electromagnets are used for measurements of Kerr magnetooptic effects [31]. The latter are measured by a reflection of an optical beam on a sample located in the

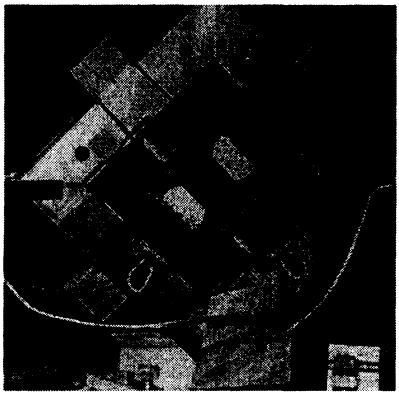

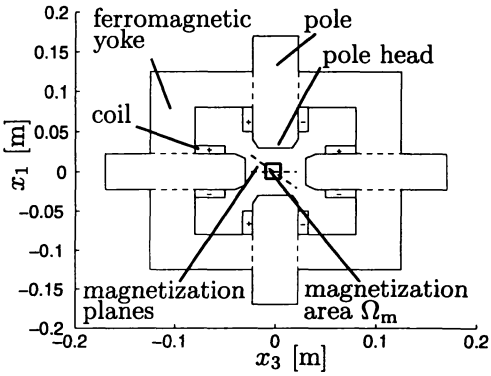

Figure 4. The Maltese Cross electromagnet and its cross-section.

magnetization area Ω_m. Here the magnetic field is required to be as homogeneous, i.e., as constant as possible in a given normal direction. Due to the anisotropy the measurements should be done in more directions, see [13], [24], [25]. Therefore, the MC electromagnet is capable of generating magnetic fields homogeneous in up to 8 directions just by switching some currents in coils on or off, or by switching their senses. Our aim is to improve the current geometry of the pole heads of the MC electromagnet such that inhomogeneities of the magnetic field are minimized, but the field itself is still strong enough.

4.2. Mathematical settings

4.2.1. Set of admissible shapes

The geometry of the MC electromagnet is depicted in Fig. 4. The dimensions are in meters. The computational domain is $\Omega := (-0.2, 0.2) \times (-0.05, 0.05) \times (-0.2, 0.2)$. We assume all the pole heads to be the same and symmetric. Then, it is enough to consider the shape α to be a quarter of the shape of the left pole head, while the symmetry with respect to the planes $x_1 = 0$ and $x_2 = 0$ will be involved in the parametrization F later on. The shape is a continuous function defined over $\omega := (0, d_{\text{pole},1}/2) \times (0, d_{\text{pole},2}/2)$, where $d_{\text{pole},1} := 0.045$, $d_{\text{pole},2} := 0.025$. Further, we choose $C_5 := \arctan(3\pi/8)$ and specify the box constraints by $\alpha_l := 0.012$, $\alpha_u := 0.05$. The pole heads cannot penetrate then. Now, the set of admissible shapes $\mathcal{U}$ is determined and Lemma 7 holds.

From the practical point of view, we cannot manufacture any shape, so we consider a Bézier patch of a fixed number of design parameters $n_\Upsilon := n_{\Upsilon,1} \cdot n_{\Upsilon,2}$, where $n_{\Upsilon,1} := 4$, $n_{\Upsilon,2} := 3$. To this end, we decompose the shape domain ω into $(n_{\Upsilon,1} - 1) \cdot (n_{\Upsilon,2} - 1)$ regular rectangles whose $n_{\Upsilon,1} \cdot n_{\Upsilon,2}$ corners are $\mathbf{x}_{\omega,i,j} := ((i-1)d_{\text{pole},1}/(n_{\Upsilon,1}-1), (j-1)d_{\text{pole},2}/(n_{\Upsilon,2}-1))$ for $i = 1, \ldots, n_{\Upsilon,1}$, $j = 1, \ldots, n_{\Upsilon,2}$.

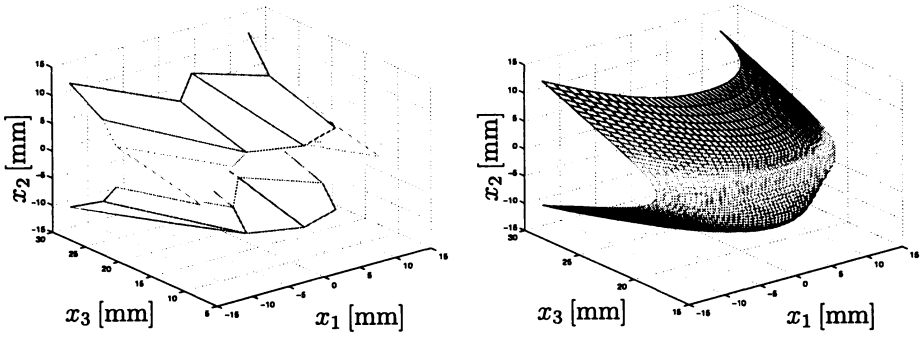

Figure 5. Bézier design parameters and the corresponding shape.

The set Υ is defined as

$$\Upsilon := \{\mathbf{p} := (p_{1,1}, \ldots, p_{n_{\Upsilon,1},n_{\Upsilon,2}}) \in \mathbb{R}^{n_\Upsilon} \mid \alpha_\mathrm{l} \leqslant p_{i,j} \leqslant \alpha_\mathrm{u}\}.$$

The mapping $F\colon \Upsilon \mapsto \mathcal{U}$, see also (14), is the following (tensor product) *Bézier mapping* that involves the symmetry assumed above:

$$\begin{aligned}\alpha(x_1, x_2) &:= [F(x_1, x_2)](\mathbf{p}) \\ &:= \sum_{i=1}^{n_{\Upsilon,1}} \sum_{j=1}^{n_{\Upsilon,2}} p_{i,j} \left[\beta_i^{2n_{\Upsilon,1}-1}\Big(\frac{-2x_1 + d_{\mathrm{pole},1}}{2d_{\mathrm{pole},1}}\Big) + \beta_i^{2n_{\Upsilon,1}-1}\Big(\frac{2x_1 + d_{\mathrm{pole},1}}{2d_{\mathrm{pole},1}}\Big)\right] \\ &\quad \times \left[\beta_j^{2n_{\Upsilon,2}-1}\Big(\frac{-2x_2 + d_{\mathrm{pole},2}}{2d_{\mathrm{pole},2}}\Big) + \beta_j^{2n_{\Upsilon,2}-1}\Big(\frac{2x_2 + d_{\mathrm{pole},2}}{2d_{\mathrm{pole},2}}\Big)\right],\end{aligned}$$

where $(x_1, x_2) \in \overline{\omega}$ and where for $n \in \mathbb{N}$, $i \in \mathbb{N}$, $i \leqslant n$, and $t \in [0, 1]$ we have

$$\beta_i^n(t) := \frac{(n-1)!}{(i-1)!\,(n-i)!} t^{i-1}(1-t)^{n-i},$$

which is called the *Bernstein polynomial.* An example of the mapping F is depicted in Fig. 5. Concerning 15, we perform the mirroring of the shape α with respect to the planes $x_1 = 0$ and $x_2 = 0$ and, moreover, copy this resulting shape to all the remaining pole heads. In this way the shape α controls the decomposition of Ω into $\Omega_0(\alpha)$ that denotes the domain occupied by the coils or air and into $\Omega_1(\alpha)$ which is the domain occupied by the yoke or poles. It is easy to see that the mapping F is continuous on Υ.

4.2.2. Multistate problem

Concerning the bilinear form, $\mu_0 := 4\pi 10^{-7}\,[\mathrm{Hm}^{-1}]$ is the air permeability and $\mu_1 := 5100\mu_0\,[\mathrm{Hm}^{-1}]$ is the permeability of the kind of steel used. We distinguish

two variations of $\mathbf{J}^v$, namely, we set $v := 1$ for a vertical variation for which only two opposite coils are pumped and $v := 2$ for a diagonal variation for which four coils are pumped as in Fig. 4. Each of the other 6 variations of the current excitation is given by a mirroring. We consider the static current $I = 5\,[\mathrm{A}]$ and 600 turns on each coil. The compatibility condition (3) is obviously fulfilled.

4.2.3. Shape optimization problem

We introduce the magnetization area $\Omega_{\mathrm{m}} := (-0.005, 0.005)^3$, see Fig. 4. The cost functional is

$$\mathcal{I}(\mathbf{u}^1(\alpha,\mathbf{x}),\mathbf{u}^2(\alpha,\mathbf{x})) := \frac{1}{2}\cdot\sum_{v=1}^{2}[\varphi^v(\mathbf{B}^v(\alpha,\mathbf{x})) + \varrho\cdot\theta^v(\mathbf{B}^v(\alpha,\mathbf{x}))],$$

where, for $v = 1, 2$, $\mathbf{B}^v(\alpha,\mathbf{x}) := \mathbf{curl}_{\mathbf{x}}(\mathbf{u}^v(\alpha,\mathbf{x}))$ is the magnetic field of the vth state problem, and where the particular contributions are defined by

$$\begin{aligned}
\varphi^v(\mathbf{B}^v(\alpha,\mathbf{x})) &:= \frac{1}{\mathrm{meas}(\Omega_{\mathrm{m}})\cdot(B^{\mathrm{avg},v}_{\mathrm{min}})^2} \\
&\quad\times\int_{\Omega_{\mathrm{m}}}\|\mathbf{B}^v(\alpha,\mathbf{x}) - B^{\mathrm{avg},v}(\mathbf{B}^v(\alpha,\mathbf{x}))\cdot\mathbf{n}^v_{\mathrm{m}}\|^2\,\mathrm{d}\mathbf{x}, \\
\theta^v(\mathbf{B}^v(\alpha,\mathbf{x})) &:= (\max\{0, B^{\mathrm{avg},v}_{\mathrm{min}} - B^{\mathrm{avg},v}(\mathbf{B}^v(\alpha,\mathbf{x}))\})^2, \quad \varrho := 10^6, \\
B^{\mathrm{avg},v}(\mathbf{B}^v(\alpha,\mathbf{x})) &:= \frac{1}{\mathrm{meas}(\Omega_{\mathrm{m}})}\cdot\int_{\Omega_{\mathrm{m}}}\|\mathbf{B}^v(\alpha,\mathbf{x})\cdot\mathbf{n}^v_{\mathrm{m}}\|\,\mathrm{d}\mathbf{x},
\end{aligned}$$

where $B^{\mathrm{avg},1}_{\mathrm{min}} = B^{\mathrm{avg},2}_{\mathrm{min}} := 0.08\,[\mathrm{T}]$, $\mathbf{n}^1_{\mathrm{m}} := (1,0,0)$, and $\mathbf{n}^2_{\mathrm{m}} := (1/\sqrt{2}, 0, 1/\sqrt{2})$. It is obvious that $\mathcal{I}$ is continuous. Now the existence of solutions to both the problems (P) and $(\widetilde{\mathrm{P}})$ follows.

Further, we choose $\varepsilon := 10^{-6}$ and $\overline{h} := 0.4$. The triangulation $\mathcal{T}^h_\omega$ of the shape domain involves the nodes $\mathbf{x}_{\omega,i,j}$. The integrals involved in the cost functional are replaced by the corresponding sums over elements.

4.3. Numerical results

The problem is solved using scientific software tools [15], [19], [28]. They have been developed within SFB F013 at the University of Linz, Austria. The resulting linear systems are solved by a preconditioned conjugate gradient method. In case the number of design variables is small, a direct solver is applied. Concerning optimization, we use the sequential quadratic programming (SQP) with an updating formulae of the Hessian matrix. The gradient is calculated by the adjoint method. Moreover, we have introduced and used a multilevel optimization approach the idea of which is to use the SQP within a hierarchy of discretizations of the optimization problem such

that a coarse optimized design is prolonged and used as the initial guess at the next finer level. In [20] we have shown that using the multilevel approach significantly reduces the computational time.

The 3d optimized shape is described by 12 design variables and was solved in 93 SQP iterations which took almost 30 hours. The underlying discretized 3d state problem has 29541 unknowns. The 2d and 3d resulting shapes are depicted in Fig. 6, where the reduced 2d problem has arisen by neglecting the dimension x_2. The initial design is depicted in Fig. 4. Some 2d and preliminary 3d numerical results, as well as various details, are presented in [16], [18].

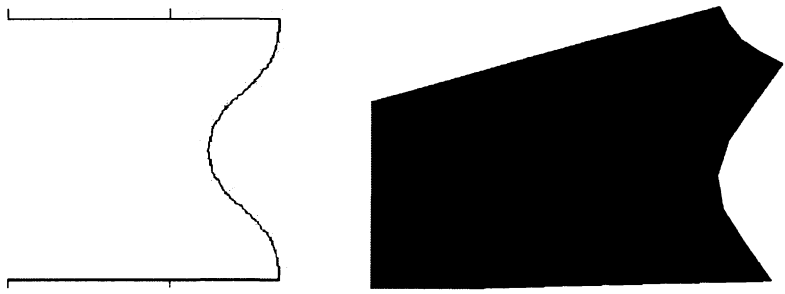

Figure 6. 2d and 3d optimized pole heads of the MC electromagnet.

4.4. Manufacture and measurements

After the 2d optimized shape, see Fig. 6, the pole heads were manufactured and the magnetic field was measured. In Fig. 7 the related distributions of the normal component of the magnetic flux density are depicted. We can see a significant improvement of the homogeneity of the magnetic field. The cost functional calculated from the measured data decreased 4.5-times. Nevertheless, the magnitude of the magnetic field decreased as well. Choosing a proper compromise between the homogeneity and the strength of the magnetic field is a difficult engineering task. Moreover, the relative differences between the measured and the calculated magnetic fields are about 30 %, which might be caused by saturation of the magnetic field in the corners. Employing a nonlinear governing magnetostatic state problem should improve this mismatch.

5. Conclusions

This paper treated the shape optimization in three-dimensional linear magnetostatics. We have met one serious obstacle, see Remark 1, that we can hardly find a continuous mapping between the shape design nodes and the remaining nodes in the discretization grid. For fine discretizations and large changes in the design shape

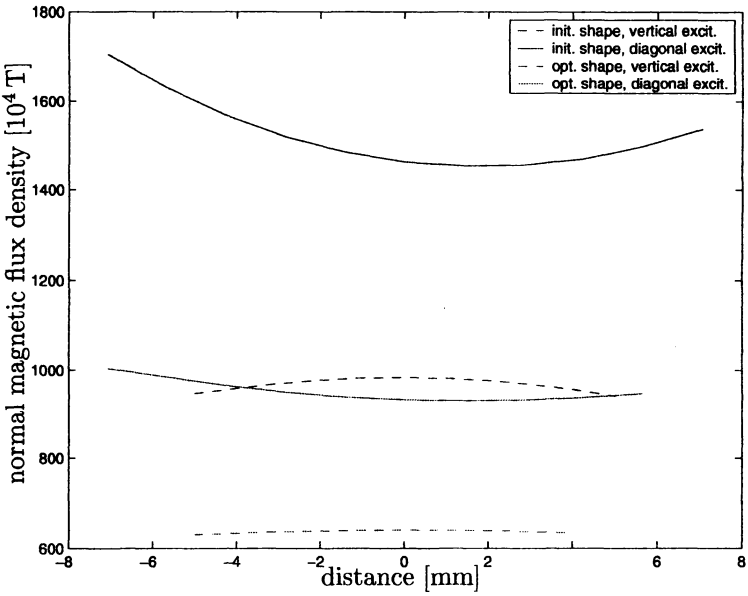

Figure 7. Magnetic field for the initial and the optimized design.

some elements flip. One possible solution consists in the use of the multilevel optimization techniques, where on the fine grids the difference between the initial and optimized shapes is not that big. Another one might be when using composite finite elements that were developed for the treatment with complicated geometries in the papers [8], [9]. It is also connected to fictitious domain methods, cf. [10]. We can also avoid this problem by using a boundary element discretization. However, construction of efficient multigrid solvers as well as using the method for nonlinear governing state problems are still topics of the current research.

References

[1] *D. Begis, R. Glowinski*: Application de la méthode des éléments finis à la résolution d'un problème de domaine optimal. Méthodes de résolution des problèmes. Appl. Math. Optim. *2* (1975), 130–169. (In French.)

[2] *A. Bossavit*: Computational Electromagnetism. Variational Formulations, Complementarity, Edge Elements. Academic Press, Orlando, 1998.

[3] *D. Braess*: Finite Elements. Theory, Fast Solvers, and Applications in Solid Mechanics. Cambridge University Press, Cambridge, 2001.

[4] *J. Chleboun, R. Mäkinen*: Primal hybrid formulation of an elliptic equation in smooth optimal shape problems. Adv. Math. Sci. Appl. *5* (1995), 139–162.

[5] *P. Doktor*: On the density of smooth functions in certain subspaces of Sobolev spaces. Comment. Math. Univ. Carolin. *14* (1973), 609–622.

[6] *G. E. Farin*: Curves and Surfaces for Computer-Aided Geometric Design: A Practical Guide. Academic Press, Boston, 1997.

[7] *V. Girault, P.-A. Raviart*: Finite Element Methods for Navier-Stokes equations. Theory and Algorithms. Springer-Verlag, Berlin, 1986.

[8] *W. Hackbusch, S. A. Sauter*: Composite finite elements for the approximation of PDEs on domains with complicated micro-structures. Numer. Math. *75* (1997), 447–472.

[9] *W. Hackbusch, S. A. Sauter*: Composite finite elements for problems containing small geometric details. II: Implementation and numerical results. Comput. Vis. Sci. *1* (1997), 15–25.

[10] *J. Haslinger, T. Kozubek*: A fictitious domain approach for a class of Neumann boundary value problems with applications in shape optimization. East-West J. Numer. Math. *8* (2000), 1–23.

[11] *J. Haslinger, P. Neittaanmäki*: Finite Element Approximation for Optimal Shape, Material and Topology Design, 2nd ed. Wiley, Chichester, 1996.

[12] *R. Hiptmair*: Multilevel preconditioning for mixed problems in three dimensions. PhD. thesis. University of Augsburg, 1996.

[13] *I. Kopřiva, D. Hrabovský, K. Postava, D. Ciprian, and J. Pištora*: Anisotropy of the quadratic magneto-optical effects in a cubic crystal. Proceedings of SPIE, Vol. 4016. 2000, pp. 54–59.

[14] *M. Křížek, P. Neittaanmäki*: Mathematical and Numerical Modelling in Electrical Engineering. Theory and Practice. Kluwer Academic Publishers, Dordrecht, 1996.

[15] *M. Kuhn, U. Langer, and J. Schöberl*: Scientific computing tools for 3d magnetic field problems. In: The Mathematics of Finite Elements and Applications. Proceedings of the 10th conference MAFELAP, 1999 (J R. Whiteman, ed.). 2000, pp. 239–258.

[16] *D. Lukáš*: Shape optimization of homogeneous electromagnets. Scientific Computing in Electrical Engineering. Lect. Notes Comput. Sci. Eng. Vol. 18 (U. van Rienen, M. Günther, and D. Hecht, eds.). 2001, pp. 145–152.

[17] *D. Lukáš*: Optimal Shape Design in Magnetostatics. PhD. thesis. VŠB-Technical University, Ostrava, 2003.

[18] *D. Lukáš, I. Kopřiva, D. Ciprian, and J. Pištora*: Shape optimization of homogeneous electromagnets and their application to measurements of magnetooptic effects. Records of COMPUMAG (2001), 156–157.

[19] *D. Lukáš, W. Mühlhuber, and M. Kuhn*: An object-oriented library for the shape optimization problems governed by systems of linear elliptic partial differential equations. Transactions of the VŠB-Technical University Ostrava *1* (2001), 115–128.

[20] *D. Lukáš, D. Ciprian, J. Pištora, K. Postava, and M. Foldyna*: Multilevel solvers for 3-dimensional optimal shape design with an application to magneto-optics. Proceedings of the 9th International Symposium on Microwave and Optical Technology (ISMOT 2003, Ostrava), SPIE Vol. 5445. 2004, pp. 235–239.

[21] *J. Lukeš, J. Malý*: Measure and Integral. MATFYZPRESS, Praha, 1995.

[22] *J. C. Nédélec*: Mixed finite elements in $\mathbb{R}^3$. Numer. Math. *35* (1980), 315–341.

[23] *O. Pironneau*: Optimal Shape Design for Elliptic Systems. Springer Series in Computational Physics. Springer-Verlag, New York, 1984.

[24] *J. Pištora, K. Postava, and R. Šebesta*: Optical guided modes in sandwiches with ultrathin metallic films. Journal of Magnetism and Magnetic Materials *198–199* (1999), 683–685.

[25] *K. Postava, D. Hrabovský, J. Pištora, A. R. Fert, Š. Višňovský, and T. Yamaguchi*: Anisotropy of quadratic magneto-optic effects in reflection. J. Appl. Phys. *91* (2002), 7293–7295.

[26] *P.-A. Raviart and J. M. Thomas*: A mixed finite element method for second order elliptic problems. Lecture Notes in Math. *606* (1977), 292–315.

[27] *S. Reitzinger, J. Schöberl*: An algebraic multigrid method for finite element discretizations with edge elements. Numer. Linear Algebra Appl. *9* (1997), 223–238.
[28] *J. Schöberl*: NETGEN: An advancing front 2D/3D-mesh generator based on abstract rules. Comput. Vis. Sci. *1* (1997), 41–52.
[29] *N. Takahashi*: Optimization of die press model. Proceedings of the TEAM Workshop in the Sixth Round (Okayama, Japan), March 1996.
[30] *U. van Rienen*: Numerical methods in computational electrodynamics. Linear Systems in Practical Applications, Lect. Notes Comp. Sci. Engrg. Vol. 12. Springer-Verlag, Berlin, 2001.
[31] *A. K. Zvedin, V. A. Kotov*: Modern Magnetooptics and Magnetooptical Materials. Institute of Physics Publishing, Bristol and Philadelphia, 1997.

Author's address: *D. Lukáš*, Department of Applied Mathematics (K457), VŠB-Technical University of Ostrava, 17. listopadu 15, 708 33 Ostrava-Poruba, Czech Republic, e-mail: `dalibor.lukas@vsb.cz`.

49 (2004) APPLICATIONS OF MATHEMATICS No. 5, 441–464

ON SOLUTION TO AN OPTIMAL SHAPE DESIGN PROBLEM IN 3-DIMENSIONAL LINEAR MAGNETOSTATICS*

Dalibor Lukáš, Ostrava

(Received September 9, 2002, in revised version January 15, 2004)

Abstract. In this paper we present theoretical, computational, and practical aspects concerning 3-dimensional shape optimization governed by linear magnetostatics. The state solution is approximated by the finite element method using Nédélec elements on tetrahedra. Concerning optimization, the shape controls the interface between the air and the ferromagnetic parts while the whole domain is fixed. We prove the existence of an optimal shape. Then we state a finite element approximation to the optimization problem and prove the convergence of the approximated solutions. In the end, we solve the problem for the optimal shape of an electromagnet that arises in the research on magnetooptic effects and that was manufactured afterwards.

Keywords: optimal shape design, finite element method, magnetostatics, magnetooptics

MSC 2000: 49J20, 65K10, 35J40, 65N30

1. Introduction

In the paper we present 3-dimensional (3d) shape optimization of an electromagnet arising in the research on magnetooptic effects. A useful framework for the existence and convergence proofs is given by an abstract theory in [11] together with applications mostly in mechanics. Our theory differs mainly by the fact that the optimized shape controls the interface between the air and the ferromagnetic parts, rather than the whole domain boundary, as it is usual in mechanics. The domain is fixed in our

* This research has been supported by the Austrian Science Fund FWF within the SFB "Numerical and Symbolic Scientific Computing" under grant SFB F013, by the Czech Ministry of Education under research project CEZ: J17/98:272400019, and by the Grant Agency of the Czech Republic under grant 105/99/1698.

case. Variational formulations of the magnetostatic problem and their finite element discretizations are given in [2], [14], [30] using the space $\mathbf{H}(\mathbf{curl})$ that was well described in [7], [22]. Some shape optimization problems governed by 2-dimensional (2d) nonlinear magnetostatics are treated in [23], [29].

The paper is organized as follows. In Section 2 we introduce a weak formulation of linear magnetostatics in $\mathbf{H_0}(\mathbf{curl})/\,\mathbf{Ker_0}(\mathbf{curl})$ and prove the existence and uniqueness of the solution. Further, we regularize the bilinear form due to its nonellipticity and prove the convergence of the regularized solutions. Finally, we discretize the problem by the finite element method using the first-order Nédélec tetrahedral elements and prove the convergence. In Section 3 we introduce a shape optimization problem. We prove the compactness of the set of admissible shapes and the continuity of the cost functional. We regularize the bilinear form, employ the finite element discretization, and prove the convergence of the optimized discretized shapes. Finally, we make notes on the first-order sensitivity analysis. In Section 4 the theory is applied to optimal shape design of an electromagnet. We give a 3d optimized shape as well as a 2d one which resulted from a dimensionally reduced formulation. According to the 2d optimized shape, pole heads of the electromagnet were manufactured and we discuss the improvements in terms of physical measurements of the magnetic field before and after optimization.

2. Three-dimensional linear magnetostatics

Assumption 1. In all what follows let $\Omega \subset \mathbb{R}^3$ be a nonempty bounded convex domain with a polyhedral boundary.

2.1. Linear magnetostatics

Let $\mathbf{B}$ and $\mathbf{J}$ denote the magnetic field and the current density, respectively. We introduce the magnetic vector potential $\mathbf{u}$ by

$$\mathbf{curl}(\mathbf{u}) = \mathbf{B}.$$

We consider the following magnetostatic boundary value problem:

$$\text{(S)} \qquad \begin{cases} \mathbf{curl}\Big(\dfrac{1}{\mu}\,\mathbf{curl}(\mathbf{u})\Big) = \mathbf{J} & \text{in } \Omega \\ \mathbf{n} \times \mathbf{u} = \mathbf{0} & \text{on } \partial\Omega \end{cases}$$

We suppose that only the air and the ferromagnetics occupy Ω, i.e., there exists a decomposition of Ω into subdomains Ω_0 and Ω_1 such that

$$\overline{\Omega} = \overline{\Omega_0} \cup \overline{\Omega_1}, \quad \Omega_0 \cap \Omega_1 = \emptyset, \quad \text{and} \quad \operatorname{meas}(\Omega_0), \operatorname{meas}(\Omega_1) \neq 0,$$

where meas stands for the Lebesgue measure and we suppose that there exist constants μ_0, μ_1 such that

$$0 < \mu_0 < \mu_1, \quad \mu|_{\Omega_0} = \mu_0, \quad \text{and} \quad \mu|_{\Omega_1} = \mu_1. \tag{1}$$

2.2. The space H(curl)

We will extend the differential operator **curl** to a subspace of $[L^2(\Omega)]^3$. A function $\mathbf{z} \in [L^2(\Omega)]^3$ is called the *generalized rotation* of $\mathbf{u} \in [L^2(\Omega)]^3$ if

$$\forall\, \mathbf{v} \in [C_0^\infty(\Omega)]^3 \colon \int_\Omega \mathbf{u} \cdot \mathbf{curl}(\mathbf{v})\, \mathrm{d}\mathbf{x} = \int_\Omega \mathbf{z} \cdot \mathbf{v}\, \mathrm{d}\mathbf{x}$$

and we denote the generalized rotation by $\mathbf{curl}(\mathbf{u}) := \mathbf{z}$. We define the space

$$\mathbf{H}(\mathbf{curl}; \Omega) := \{\mathbf{u} \in [L^2(\Omega)]^3 \mid \exists\, \mathbf{z} \in [L^2(\Omega)]^3 \colon\ \mathbf{z} = \mathbf{curl}(\mathbf{u})\}$$

which together with the scalar product

$$(\mathbf{u}, \mathbf{v})_{\mathbf{curl},\Omega} := \int_\Omega \mathbf{u} \cdot \mathbf{v}\, \mathrm{d}\mathbf{x} + \int_\Omega \mathbf{curl}(\mathbf{u}) \cdot \mathbf{curl}(\mathbf{v})\, \mathrm{d}\mathbf{x}$$

forms a Hilbert space. We introduce the induced norm and seminorm by

$$\|\mathbf{u}\|_{\mathbf{curl},\Omega} := \sqrt{(\mathbf{u}, \mathbf{u})_{\mathbf{curl},\Omega}} \quad \text{and} \quad |\mathbf{u}|_{\mathbf{curl},\Omega} := \sqrt{\int_\Omega \|\,\mathbf{curl}(\mathbf{u})\|^2\, \mathrm{d}\mathbf{x}},$$

where $\|\cdot\|$ denotes the Euclidean norm.

Due to [7, p. 34], the operator $\mathbf{n} \times \mathbf{u}|_{\partial\Omega}$ can be extended by continuity onto the space $\mathbf{H}(\mathbf{curl}; \Omega)$. Thus, the following spaces are well-defined:

$$\mathbf{H_0}(\mathbf{curl}; \Omega) := \{\mathbf{u} \in \mathbf{H}(\mathbf{curl}; \Omega) \mid \mathbf{n} \times \mathbf{u} = \mathbf{0} \ \text{ on } \ \partial\Omega\},$$
$$\mathbf{Ker_0}(\mathbf{curl}; \Omega) := \{\mathbf{u} \in \mathbf{H_0}(\mathbf{curl}; \Omega) \mid \mathbf{curl}(\mathbf{u}) = \mathbf{0} \ \text{ in } \ \Omega\}.$$

The quotient space $\mathbf{H_0}(\mathbf{curl}; \Omega)/\,\mathbf{Ker_0}(\mathbf{curl}; \Omega)$ will be used as the test space for a weak formulation of (S). By [12, p. 94–95] it is isomorphically isometric to

$$\mathbf{H}_{\mathbf{0},\perp}(\mathbf{curl}; \Omega) := \left\{\mathbf{u} \in \mathbf{H_0}(\mathbf{curl}; \Omega) \mid \forall\, p \in H_0^1(\Omega) \colon \int_\Omega \mathbf{u} \cdot \mathbf{grad}(p)\, \mathrm{d}\mathbf{x} = 0\right\}.$$

Moreover, we have the orthogonal decomposition

$$\mathbf{H_0}(\mathbf{curl}; \Omega) = \mathbf{H}_{\mathbf{0},\perp}(\mathbf{curl}; \Omega) \oplus \mathbf{Ker_0}(\mathbf{curl}; \Omega).$$

The following densities hold in the norm $\|\cdot\|_{\mathbf{curl},\Omega}$:

$$\mathbf{H}(\mathbf{curl}; \Omega) = \overline{[C^\infty(\overline{\Omega})]^3} \quad \text{and} \quad \mathbf{H_0}(\mathbf{curl}; \Omega) = \overline{[C_0^\infty(\Omega)]^3}. \tag{2}$$

Finally, we will make use of a Friedrichs'-like inequality:

Lemma 1. *There exists a positive constant C_1 such that*

$$\forall\, \mathbf{v} \in \mathbf{H}_{\mathbf{0},\perp}(\mathbf{curl};\Omega)\colon\ \|\mathbf{v}\|_{\mathbf{curl},\Omega} \leqslant C_1 |\mathbf{v}|_{\mathbf{curl},\Omega}.$$

P r o o f. See [12, p. 96]. □

2.3. Weak formulation

We introduce a bilinear form a and a linear functional f, both related to (S), by

$$a(\mathbf{v},\mathbf{u}) := \int_{\Omega_0} \frac{1}{\mu_0}\mathbf{curl}(\mathbf{v})\cdot\mathbf{curl}(\mathbf{u})\,\mathrm{d}\mathbf{x} + \int_{\Omega_1} \frac{1}{\mu_1}\mathbf{curl}(\mathbf{v})\cdot\mathbf{curl}(\mathbf{u})\,\mathrm{d}\mathbf{x},$$
$$f(\mathbf{v}) := \int_{\Omega} \mathbf{J}\cdot\mathbf{v}\,\mathrm{d}\mathbf{x}, \quad \mathbf{u},\mathbf{v} \in \mathbf{H}(\mathbf{curl};\Omega),$$

where the current density $\mathbf{J} \in [L^2(\Omega)]^3$ satisfies the compatibility condition

$$(3)\quad \forall\, \mathbf{w} \in \mathbf{Ker_0}(\mathbf{curl};\Omega)\colon\ f(\mathbf{w}) = 0, \quad \text{i.e.,} \quad \forall\, p \in H_0^1(\Omega)\colon \int_{\Omega} \mathbf{J}\cdot\mathbf{grad}(p)\,\mathrm{d}\mathbf{x} = 0.$$

Then, the weak formulation of (S) reads as follows:

$$(\mathrm{W}) \qquad \begin{cases} \text{Find } \ \mathbf{u} \in \mathbf{H}_{\mathbf{0},\perp}(\mathbf{curl};\Omega)\colon \\ a(\mathbf{v},\mathbf{u}) = f(\mathbf{v}) \ \ \forall\, \mathbf{v} \in \mathbf{H}_{\mathbf{0},\perp}(\mathbf{curl};\Omega). \end{cases}$$

Lemma 2. *There exists a unique solution $\mathbf{u} \in \mathbf{H}_{\mathbf{0},\perp}(\mathbf{curl};\Omega)$ to* (W).

P r o o f. It is easy to see that the space $\mathbf{H}_{\mathbf{0},\perp}(\mathbf{curl};\Omega)$ equipped with the scalar product $(\cdot,\cdot)_{\mathbf{curl},\Omega}$ forms a Hilbert space and that the linear functional f and the bilinear form a are bounded. The ellipticity of a on $\mathbf{H}_{\mathbf{0},\perp}(\mathbf{curl};\Omega)$ follows from

$$(4)\qquad a(\mathbf{v},\mathbf{v}) \geqslant \frac{1}{\mu_1}\int_{\Omega} \|\,\mathbf{curl}(\mathbf{v})\|^2\,\mathrm{d}\mathbf{x} = \frac{1}{\mu_1}|\mathbf{v}|^2_{\mathbf{curl},\Omega} \geqslant \frac{1}{\mu_1 C_1^2}\|\mathbf{v}\|^2_{\mathbf{curl},\Omega},$$

where we have used (1) and Lemma 1. The statement now follows directly from the Lax-Milgram lemma, cf. [14, p. 14]. □

2.4. Regularization of the bilinear form

The problem (W) is equivalent to a mixed variational formulation. We will rather introduce a non-mixed formulation in $\mathbf{H_0}(\mathbf{curl};\Omega)$ while we regularize the nonellipticity of a. The solutions will then tend towards the solution of (W).

Let $\varepsilon > 0$ be a regularization parameter by which we regularize a:

$$a_\varepsilon(\mathbf{v}, \mathbf{u}) := a(\mathbf{v}, \mathbf{u}) + \varepsilon \int_\Omega \mathbf{v} \cdot \mathbf{u} \, \mathrm{d}\mathbf{x}, \quad \mathbf{u}, \mathbf{v} \in \mathbf{H}(\mathbf{curl}; \Omega).$$

The regularized weak formulation then reads

$$(\mathrm{W}_\varepsilon) \qquad \begin{cases} \text{Find } \mathbf{u}_\varepsilon \in \mathbf{H_0}(\mathbf{curl}; \Omega): \\ a_\varepsilon(\mathbf{v}, \mathbf{u}_\varepsilon) = f(\mathbf{v}) \quad \forall \, \mathbf{v} \in \mathbf{H_0}(\mathbf{curl}; \Omega), \end{cases}$$

where we still assume that (3) holds.

For each $\varepsilon > 0$ we can easily prove the existence of a unique solution $\mathbf{u}_\varepsilon$ to (W_ε). The following lemma gives a convergence property:

Lemma 3. *The following convergence holds:*

$$\mathbf{u}_\varepsilon \to \mathbf{u} \ \textit{in} \ \mathbf{H_0}(\mathbf{curl}; \Omega) \ \textit{as} \ \varepsilon \to 0_+,$$

where $\mathbf{u}_\varepsilon$ *are the solutions to* (W_ε) *and* $\mathbf{u}$ *is the solution to* (W).

P r o o f. See [27, Lemma 2.1]. □

2.5. Finite element approximation

We denote by $\mathcal{T}^h := \{K^{e_i} \mid i = 1, \dots, n_\Omega\}$ a face-to-face discretization of Ω into tetrahedra. Let h^e denote the length of the shortest edge of a tetrahedron K^e. We denote by $h := \min\limits_{K^e \in \mathcal{T}^h} h^e$ the discretization parameter. Clearly, there exists $\overline{h} > 0$ being the maximal size in the geometry such that $h \leqslant \overline{h}$.

2.5.1. Discretization of the test space using Nédélec elements

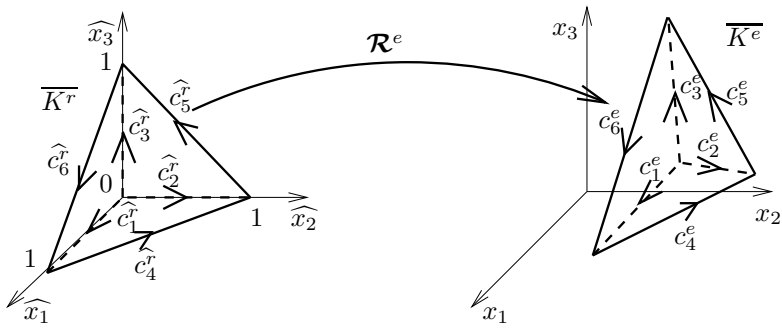

Figure 1. A transformation from the reference Nédélec tetrahedron.

The *linear Nédélec element* is a triple $E := (\overline{K^e}, \mathbf{P}^e, \Sigma^e)$, where $K^e \subset \mathbb{R}^3$ is a tetrahedral domain,

$$\mathbf{P}^e := \{\mathbf{p}(\mathbf{x}) := \mathbf{a}^e \times \mathbf{x} + \mathbf{b}^e \mid \mathbf{a}^e, \mathbf{b}^e \in \mathbb{R}^3, \ \ \mathbf{x} := (x_1, x_2, x_3) \in \overline{K^e}\},$$

and $\Sigma^e := \{\sigma_1^e, \ldots, \sigma_6^e\}$, where the degree of freedom is defined by

$$\sigma_i^e(\mathbf{v}) := \int_{c_i^e} \mathbf{v} \cdot \mathbf{t}_i^e \, \mathrm{d}\mathbf{s}, \quad i = 1, \ldots, 6,$$

where c_i^e stand for oriented edges, see Fig. 1, and $\mathbf{t}_i^e$ are the related unit tangential vectors. By [22, Th. 1], this element is $\mathbf{H}(\mathbf{curl}; K^e)$-conforming.

By $\boldsymbol{\xi}_1^e, \ldots, \boldsymbol{\xi}_6^e \in \mathbf{P}^e$ we denote the shape functions related to the element K^e. In a standard way we introduce the global shape functions $\boldsymbol{\xi}_1^h, \ldots, \boldsymbol{\xi}_n^h \colon \overline{\Omega} \mapsto \mathbb{R}^3$, where n is the number of edges (degrees of freedom) in the discretization $\mathcal{T}^h$. We introduce a conforming approximation of $\mathbf{H_0}(\mathbf{curl}; \Omega)$ by

$$\mathbf{H_0}(\mathbf{curl}; \Omega)^h := \left\{ \mathbf{v}^h = \sum_{\mathbf{n} \times \boldsymbol{\xi}_i^h = \mathbf{0}} v_i^h \boldsymbol{\xi}_i^h \mid v_i^h \in \mathbb{R} \right\}.$$

It can be easily seen that $\mathbf{H_0}(\mathbf{curl}; \Omega)^h \subset \mathbf{H_0}(\mathbf{curl}; \Omega)$, see [17].

The linear transformation $\boldsymbol{\mathcal{R}}^e(\hat{\mathbf{x}}) := \mathbf{R}^e \cdot \hat{\mathbf{x}} + \mathbf{r}^e$ in Fig. 1 is determined by

$$\mathbf{R}^e := \begin{pmatrix} x_{2,1}^e - x_{1,1}^e & x_{3,1}^e - x_{1,1}^e & x_{4,1}^e - x_{1,1}^e \\ x_{2,2}^e - x_{1,2}^e & x_{3,2}^e - x_{1,2}^e & x_{4,2}^e - x_{1,2}^e \\ x_{2,3}^e - x_{1,3}^e & x_{3,3}^e - x_{1,3}^e & x_{4,3}^e - x_{1,3}^e \end{pmatrix}, \quad \mathbf{r}^e := \begin{pmatrix} x_{1,1}^e \\ x_{1,2}^e \\ x_{1,3}^e \end{pmatrix},$$

where $\mathbf{x}_i^e := (x_{i,1}^e, x_{i,2}^e, x_{i,3}^e)$, $i = 1, \ldots, 4$, are the corners of the tetrahedron $\overline{K^e}$ which correspond to the corners of $\overline{K^r}$:

$$\widehat{\mathbf{x}_1^r} := (0,0,0), \quad \widehat{\mathbf{x}_2^r} := (1,0,0), \quad \widehat{\mathbf{x}_3^r} := (0,1,0), \quad \widehat{\mathbf{x}_4^r} := (0,0,1).$$

The following Piola's transformation holds, see [26, Form. 3.17]:

$$\mathbf{curl}_{\mathbf{x}}(\mathbf{v}(\mathbf{x})) = \frac{1}{\det(\mathbf{R}^e)} \mathbf{R}^e \cdot \mathbf{curl}_{\hat{\mathbf{x}}}(\hat{\mathbf{v}}(\hat{\mathbf{x}})), \tag{5}$$

where $\mathbf{v}(\mathbf{x})$ and $\hat{\mathbf{v}}(\hat{\mathbf{x}})$ respectively stand for functions defined over K^e and K^r. The reference shape functions are:

$$\begin{aligned} &\widehat{\boldsymbol{\xi}_1^r}(\hat{\mathbf{x}}) := (0,-1,1) \times (\hat{\mathbf{x}}) + (1,0,0), && \widehat{\boldsymbol{\xi}_2^r}(\hat{\mathbf{x}}) := (1,0,-1) \times (\hat{\mathbf{x}}) + (0,1,0), \\ &\widehat{\boldsymbol{\xi}_3^r}(\hat{\mathbf{x}}) := (-1,1,0) \times (\hat{\mathbf{x}}) + (0,0,1), && \widehat{\boldsymbol{\xi}_4^r}(\hat{\mathbf{x}}) := (0,0,1) \times (\hat{\mathbf{x}}), \\ &\widehat{\boldsymbol{\xi}_5^r}(\hat{\mathbf{x}}) := (1,0,0) \times (\hat{\mathbf{x}}), && \widehat{\boldsymbol{\xi}_6^r}(\hat{\mathbf{x}}) := (0,1,0) \times (\hat{\mathbf{x}}), \end{aligned} \tag{6}$$

where $\hat{\mathbf{x}} := (\widehat{x_1}, \widehat{x_2}, \widehat{x_3}) \in \overline{K^r}$ and $\overline{K^r}$ is the reference tetrahedron, see Fig. 1.

Now, we will state the element approximation property. To this end we introduce an interpolation operator $\boldsymbol{\pi}^e\colon\ [C^\infty(\overline{K^e})]^3 \mapsto \mathbf{P}^e$ such that

$$\sigma_i^e(\boldsymbol{\pi}^e(\mathbf{v})) = \sigma_i^e(\mathbf{v}), \quad i = 1, \ldots, 6,$$

holds for any $\mathbf{v} \in [C^\infty(\overline{K^e})]^3$. Further, we introduce a global interpolation operator $\boldsymbol{\pi}^h\colon\ [C^\infty(\overline{\Omega})]^3 \mapsto \mathbf{H}(\mathbf{curl};\Omega)$ such that for any $\mathbf{v} \in [C^\infty(\overline{\Omega})]^3$ we have

$$\boldsymbol{\pi}^h(\mathbf{v})|_{K^e} := \boldsymbol{\pi}^e(\mathbf{v}|_{K^e}), \quad K^e \in \mathcal{T}^h.$$

The following definition and lemma are due to [22, p. 327].

Definition 1. A family $\mathcal{F} := \{\mathcal{T}^h \mid 0 < h \leqslant \overline{h}\}$ of decompositions (discretizations) of Ω into tetrahedra is said to be regular if there exists a constant $C_2 > 0$ such that for any $\mathcal{T}^h \in \mathcal{F}$ and any $K^e \in \mathcal{T}^h$ we have

$$\frac{h^e}{\varrho^e} \leqslant C_2, \tag{7}$$

where ϱ^e denotes the radius of the largest sphere inscribed in K^e.

Lemma 4. *Let $\mathcal{F}$ be a regular family of decompositions into tetrahedra in the sense of Definition* 1. *Then there exists a constant $C_3 > 0$ such that for any $\mathcal{T}^h \in \mathcal{F}$ we have*

$$\forall\, \mathbf{v} \in [C^\infty(\overline{\Omega})]^3\colon\ \|\mathbf{v} - \boldsymbol{\pi}^h(\mathbf{v})\|_{\mathbf{curl},\Omega} \leqslant C_3 h |\mathbf{v}|_{[H^2(\Omega)]^3}.$$

P r o o f. The assertion is a direct consequence of [22, Th. 2]. □

Lemma 5. *Let $\mathbf{v} \in [C_0^\infty(\Omega)]^3$ and let $\mathcal{F}$ be a regular family of decompositions. Then there exists a positive constant $C_4 \equiv C_4(\mathbf{v})$ such that for any $\mathcal{T}^h \in \mathcal{F}$ the following holds:*

$$\forall\, K^e \in \mathcal{T}^h\ \forall\, \mathbf{x} \equiv \boldsymbol{\mathcal{R}}^e(\hat{\mathbf{x}}) \in \overline{K^e}\colon\ \|\mathbf{curl}_{\mathbf{x}}(\boldsymbol{\pi}^e(\mathbf{v}|_{\overline{K^e}}))\| \leqslant C_4.$$

P r o o f. Let $\mathbf{v} \in [C_0^\infty(\Omega)]^3$ be an arbitrary function, $\mathcal{T}^h$ a regular discretization of Ω, and $K^e \in \mathcal{T}^h$ an element domain. The rotations of the reference shape functions, see (6), are constant over $\overline{K^r}$, e.g., $\mathbf{curl}_{\hat{\mathbf{x}}}(\widehat{\boldsymbol{\xi}}_1^r(\hat{\mathbf{x}})) = (0, -2, 2)$. Let us denote

$\sigma_i^e := \sigma_i^e(\mathbf{v}|_{\overline{K^e}})$ for $i = 1, 2, \ldots, 6$. Now, an application of the Stokes theorem yields

$$\mathbf{curl}_{\mathbf{x}}(\boldsymbol{\pi}^e(\mathbf{v}|_{\overline{K^e}}(\mathbf{x}))) = \frac{1}{\det(\mathbf{R}^e)} \sum_{i=1}^{6} \sigma_i^e(\mathbf{v}|_{\overline{K^e}}) \mathbf{R}^e \cdot \mathbf{curl}_{\hat{\mathbf{x}}}(\widehat{\boldsymbol{\xi}}_i^r(\hat{\mathbf{x}})) = \frac{2}{6\,\mathrm{meas}(K^e)}$$
$$\times \begin{pmatrix} (x_{2,1}^e - x_{1,1}^e)(\sigma_2^e - \sigma_3^e + \sigma_5^e) + (x_{3,1}^e - x_{1,1}^e)(\sigma_3^e - \sigma_1^e + \sigma_6^e) + (x_{4,1}^e - x_{1,1}^e)(\sigma_1^e - \sigma_2^e + \sigma_4^e) \\ (x_{2,2}^e - x_{1,2}^e)(\sigma_2^e - \sigma_3^e + \sigma_5^e) + (x_{3,2}^e - x_{1,2}^e)(\sigma_3^e - \sigma_1^e + \sigma_6^e) + (x_{4,2}^e - x_{1,2}^e)(\sigma_1^e - \sigma_2^e + \sigma_4^e) \\ (x_{2,3}^e - x_{1,3}^e)(\sigma_2^e - \sigma_3^e + \sigma_5^e) + (x_{3,3}^e - x_{1,3}^e)(\sigma_3^e - \sigma_1^e + \sigma_6^e) + (x_{4,3}^e - x_{1,3}^e)(\sigma_1^e - \sigma_2^e + \sigma_4^e) \end{pmatrix}$$
$$= \frac{-1}{3\,\mathrm{meas}(K^e)} \mathbf{R}^e \cdot \begin{pmatrix} \int_{f_2^e} \mathbf{curl}_{\mathbf{x}}(\mathbf{v}|_{\overline{K^e}}(\mathbf{x})) \cdot \mathbf{n}_2^e(\mathbf{x})\,\mathrm{d}\mathbf{S} \\ \int_{f_3^e} \mathbf{curl}_{\mathbf{x}}(\mathbf{v}|_{\overline{K^e}}(\mathbf{x})) \cdot \mathbf{n}_3^e(\mathbf{x})\,\mathrm{d}\mathbf{S} \\ \int_{f_4^e} \mathbf{curl}_{\mathbf{x}}(\mathbf{v}|_{\overline{K^e}}(\mathbf{x})) \cdot \mathbf{n}_4^e(\mathbf{x})\,\mathrm{d}\mathbf{S} \end{pmatrix},$$

where f_2^e, f_3^e, f_4^e denote faces that are opposite to the nodes $\mathbf{x}_2^e$, $\mathbf{x}_3^e$, $\mathbf{x}_4^e$, respectively, and $\mathbf{n}_2^e$, $\mathbf{n}_3^e$, $\mathbf{n}_4^e$ are the outward normal vectors. From the regularity condition (7) it is obvious that $\mathrm{meas}(K^e) \geqslant \frac{4}{3}\pi(\varrho^e)^3 \geqslant \frac{4}{3}\pi(h^e/C_2)^3$. By estimating the integrals we arrive at

$$\|\mathbf{curl}_{\mathbf{x}}(\boldsymbol{\pi}^e(\mathbf{v}|_{\overline{K^e}}(\mathbf{x})))\| \leqslant \frac{3 \max_{\mathbf{x}\in\Omega} \|\mathbf{curl}_{\mathbf{x}}(\mathbf{v}(\mathbf{x}))\| (C_2)^3}{8\pi} =: C_4,$$

where we have considered $\|\mathbf{R}^e\| := \max\limits_{i,j} |x_{i,j}^e - x_{1,j}^e|$. □

2.5.2. Discretized problem

Let Ω_0^h and Ω_1^h approximate the subdomains Ω_0 and Ω_1 so that

$$\forall\, K^e \in \mathcal{T}^h\colon\ K^e \subset \Omega_0^h \quad \text{or} \quad K^e \subset \Omega_1^h$$

and let $\mu^h(\mathbf{x})$ denote a discretization of the permeability function $\mu(\mathbf{x})$. The regularized bilinear form a_ε is approximated as follows:

$$a_\varepsilon^h(\mathbf{v}, \mathbf{u}) := \int_{\Omega_0^h} \frac{1}{\mu_0} \mathbf{curl}(\mathbf{v}) \cdot \mathbf{curl}(\mathbf{u})\,\mathrm{d}\mathbf{x} + \int_{\Omega_1^h} \frac{1}{\mu_1} \mathbf{curl}(\mathbf{v}) \cdot \mathbf{curl}(\mathbf{u})\,\mathrm{d}\mathbf{x} + \varepsilon \int_\Omega \mathbf{v} \cdot \mathbf{u}\,\mathrm{d}\mathbf{x},$$

where $\mathbf{v}, \mathbf{u} \in \mathbf{H_0}(\mathbf{curl}; \Omega)$. The discretization of (W_ε) reads as follows:

$$(\mathrm{W}_\varepsilon^h) \qquad \begin{cases} \text{Find } \mathbf{u}_\varepsilon^h \in \mathbf{H_0}(\mathbf{curl}; \Omega)^h\colon \\ a_\varepsilon^h(\mathbf{v}^h, \mathbf{u}_\varepsilon^h) = f(\mathbf{v}^h) \quad \forall\, \mathbf{v}^h \in \mathbf{H_0}(\mathbf{curl}; \Omega)^h. \end{cases}$$

The existence of a unique solution can be proven similarly as in Lemma 2.

2.5.3. The convergence property

Lemma 6. *Let Assumption* 1 *hold and let us consider a regular family* $\mathcal{F}$ *of decompositions* $\mathcal{T}^h$. *Assume that*

$$|\mu^h(\mathbf{x}) - \mu(\mathbf{x})| \to 0 \quad \text{a.e. in } \Omega \text{ as } h \to 0_+. \tag{8}$$

Then for each $\varepsilon > 0$ *and* $h > 0$ *we have*

$$\mathbf{u}_\varepsilon^h \to \mathbf{u}_\varepsilon \quad \text{in } \mathbf{H_0(curl}; \Omega) \text{ as } h \to 0_+.$$

P r o o f. Let $\varepsilon > 0$ be arbitrary. The proof is based on the following first Strang's lemma, cf. [3]: There exists $C(\varepsilon) > 0$ such that for each $\mathbf{v}^h \in \mathbf{H_0(curl}; \Omega)^h$ we have

$$\begin{aligned} &\|\mathbf{u}_\varepsilon - \mathbf{u}_\varepsilon^h\|_{\mathbf{curl},\Omega} \\ &\quad \leqslant C(\varepsilon)\left\{\|\mathbf{u}_\varepsilon^h - \mathbf{v}^h\|_{\mathbf{curl},\Omega} + \frac{|a_\varepsilon(\mathbf{v}^h, \mathbf{u}_\varepsilon^h - \mathbf{v}^h) - a_\varepsilon^h(\mathbf{v}^h, \mathbf{u}_\varepsilon^h - \mathbf{v}^h)|}{\|\mathbf{u}_\varepsilon^h - \mathbf{v}^h\|_{\mathbf{curl},\Omega}}\right\}. \end{aligned} \tag{9}$$

Now, the idea of the proof is like in [14, Th. 4.16], originally in [5]. Let $\tau > 0$ be arbitrary. By virtue of (2) there exists $\widetilde{\mathbf{u}}_\varepsilon \in [C_0^\infty(\Omega)]^3$ such that

$$\|\mathbf{u}_\varepsilon - \widetilde{\mathbf{u}}_\varepsilon\|_{\mathbf{curl},\Omega} \leqslant \frac{\tau}{4C(\varepsilon)}. \tag{10}$$

In the estimate (9) we choose $\mathbf{v}^h := \boldsymbol{\pi}^h(\widetilde{\mathbf{u}}_\varepsilon)$.

The first term on the right-hand side of (9) can be estimated as follows:

$$\begin{aligned} \|\mathbf{u}_\varepsilon - \mathbf{v}^h\|_{\mathbf{curl},\Omega} &= \|\mathbf{u}_\varepsilon - \widetilde{\mathbf{u}}_\varepsilon + \widetilde{\mathbf{u}}_\varepsilon - \mathbf{v}^h\|_{\mathbf{curl},\Omega} \\ &\leqslant \frac{\tau}{4C(\varepsilon)} + \|\widetilde{\mathbf{u}}_\varepsilon - \boldsymbol{\pi}^h(\widetilde{\mathbf{u}}_\varepsilon)\|_{\mathbf{curl},\Omega} \leqslant \frac{\tau}{4C(\varepsilon)} + C_3 h|\widetilde{\mathbf{u}}_\varepsilon|_{[H^2(\Omega)]^3}, \end{aligned} \tag{11}$$

where we have used the triangle inequality, (10), and Lemma 4. The numerator of the second term on the right-hand side of (9) is

$$\begin{aligned} &|a_\varepsilon(\mathbf{v}^h, \mathbf{u}_\varepsilon^h - \mathbf{v}^h) - a_\varepsilon^h(\mathbf{v}^h, \mathbf{u}_\varepsilon^h - \mathbf{v}^h)| \\ &\quad = \left|\int_\Omega \mathbf{curl}(\mathbf{u}_\varepsilon^h - \mathbf{v}^h)\Big(\frac{1}{\mu} - \frac{1}{\mu^h}\Big)\mathbf{curl}(\mathbf{v}^h)\,\mathrm{d}\mathbf{x}\right| \\ &\quad \leqslant \|\mathbf{u}_\varepsilon^h - \mathbf{v}^h\|_{\mathbf{curl},\Omega}\sqrt{\int_\Omega \Big|\frac{1}{\mu} - \frac{1}{\mu^h}\Big|^2 \|\mathbf{curl}(\mathbf{v}^h)\|^2\,\mathrm{d}\mathbf{x}}, \end{aligned} \tag{12}$$

where the Hölder inequality has been used. Now, by Lemma 5 there exists $C_4 > 0$ such that for any h, $0 < h \leqslant \overline{h}$, and for each $\mathbf{x} \in \overline{K^e} \subset \overline{\Omega}$ we have

$$\Big|\frac{1}{\mu(\mathbf{x})} - \frac{1}{\mu^h(\mathbf{x})}\Big|\|\mathbf{curl}(\mathbf{v}^h(\mathbf{x}))\| \leqslant \Big(\frac{1}{\mu_0} - \frac{1}{\mu_1}\Big)C_4(\widetilde{\mathbf{u}}_\varepsilon),$$

where we have also used (1). Then due to (8) and the Lebesgue dominated convergence theorem, cf. [21],

$$\int_\Omega \Big|\frac{1}{\mu} - \frac{1}{\mu^h}\Big|^2 \|\mathbf{curl}(\mathbf{v}^h)\|^2 \,\mathrm{d}\mathbf{x} \to 0 \quad \text{as } h \to 0_+. \tag{13}$$

Finally, dividing the inequality (12) by $\|\mathbf{u}_\varepsilon^h - \mathbf{v}^h\|_{\mathbf{curl},\Omega}$ and combining that with (9), (11), and (13) completes the proof. □

3. Optimal shape design

3.1. Admissible shapes

Let α stand for a shape which is a continuous function over a rectangle $\omega \subset \mathbb{R}^2$. We assume that there exists a common Lipschitz constant $C_5 > 0$ and box constraints $\alpha_\mathrm{l}, \alpha_\mathrm{u} \in \mathbb{R}$. Then the set of admissible shapes is

$$\mathcal{U} := \{\alpha \in C(\overline{\omega}) \mid \forall\, \mathbf{x}, \mathbf{y} \in \overline{\omega}\colon\ |\alpha(\mathbf{x}) - \alpha(\mathbf{y})| \leqslant C_5\|\mathbf{x} - \mathbf{y}\| \quad \text{and} \quad \alpha_\mathrm{l} \leqslant \alpha(\mathbf{x}) \leqslant \alpha_\mathrm{u}\},$$

equipped with the uniform convergence $\alpha_n \to \alpha$ in $\mathcal{U}$, i.e., $\alpha_n \rightrightarrows \alpha$ as $n \to \infty$.

Lemma 7. *$\mathcal{U}$ is compact.*

Proof. It follows from Theorem of Ascoli and Arzelà, cf. [11, p. 2]. □

In Section 4 we will deal with an application where in the end we will be looking for smooth shapes, e.g., Bézier curves or patches, cf. [6], rather than for continuous ones. To this end, being inspired by [4], we introduce a parameterization, i.e., a nonempty compact set of design parameters $\Upsilon \subset \mathbb{R}^{n_\Upsilon}$, $n_\Upsilon \in \mathbb{N}$, and a continuous nonsurjective mapping

$$F\colon\ \Upsilon \mapsto \mathcal{U}. \tag{14}$$

Finally, without loss of generality we assume that the shape α controls the following decomposition of Ω into the subdomains $\Omega_0(\alpha)$ and $\Omega_1(\alpha)$:

$$\overline{\Omega} = \overline{\Omega_0(\alpha)} \cup \overline{\Omega_1(\alpha)}, \quad \Omega_0(\alpha) \cap \Omega_1(\alpha) = \emptyset \tag{15}$$
$$\text{such that } \operatorname{graph}(\alpha) \subset \partial\Omega_0(\alpha) \cap \partial\Omega_1(\alpha) \text{ and } \operatorname{meas}(\Omega_0(\alpha)), \operatorname{meas}(\Omega_1(\alpha)) > 0,$$

an example of which is depicted in Fig. 2. Recall that the graph is defined by

$$\operatorname{graph}(\alpha) := \{(x_1, x_2, y) \in \mathbb{R}^3 \mid \mathbf{x} := (x_1, x_2) \in \overline{\omega} \quad \text{and} \quad y = \alpha(\mathbf{x})\}.$$

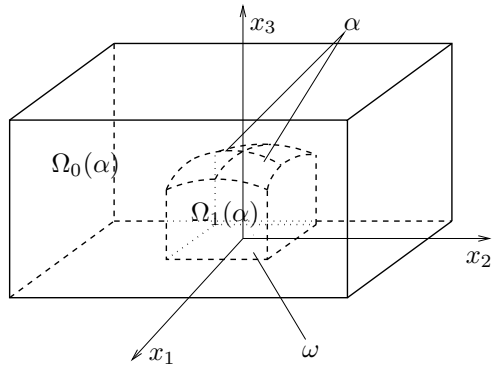

Figure 2. Decomposition of Ω.

3.2. Multistate problem

Only the piecewise constant permeability μ depends by (15) on α, thus,

$$a_\alpha(\mathbf{v},\mathbf{u}) := \int_{\Omega_0(\alpha)} \frac{1}{\mu_0}\mathbf{curl}(\mathbf{v})\cdot\mathbf{curl}(\mathbf{u})\,\mathrm{d}\mathbf{x} + \int_{\Omega_1(\alpha)} \frac{1}{\mu_1}\mathbf{curl}(\mathbf{v})\cdot\mathbf{curl}(\mathbf{u})\,\mathrm{d}\mathbf{x}.$$

Moreover, we consider n_v state problems that only differ by the current $\mathbf{J}^v$,

$$f^v(\mathbf{v}) := \int_\Omega \mathbf{J}^v\cdot\mathbf{v}\,\mathrm{d}\mathbf{x}, \quad v = 1,\dots,n_\mathrm{v},$$

so that (3) still holds. For any $\alpha\in\mathcal{U}$ and $v\in 1,\dots,n_\mathrm{v}$ we consider the following state problem, which is uniquely solvable:

$$(\mathrm{W}^v(\alpha)) \qquad \begin{cases} \text{Find } \mathbf{u}^v(\alpha)\in\mathbf{H}_{\mathbf{0},\perp}(\mathbf{curl};\Omega): \\ a_\alpha(\mathbf{v},\mathbf{u}^v(\alpha)) = f^v(\mathbf{v}) \quad \forall\,\mathbf{v}\in\mathbf{H}_{\mathbf{0},\perp}(\mathbf{curl};\Omega) \end{cases}$$

Lemma 8. *For each v the mapping $\mathbf{u}^v\colon \mathcal{U}\mapsto\mathbf{H}_{\mathbf{0},\perp}(\mathbf{curl};\Omega)$ is continuous.*

P r o o f. Let $v = 1,\dots,n_\mathrm{v}$ be arbitrary and let $\{\alpha_n\}\subset\mathcal{U}$ be a sequence such that $\alpha_n\rightrightarrows\alpha$, where $\alpha\in\mathcal{U}$. For simplicity, we set $\mathbf{u} := \mathbf{u}^v(\alpha)$ and $\mathbf{u}_n := \mathbf{u}^v(\alpha_n)$. We observe that (4) holds independently of α. Thus, by $(\mathrm{W}^v(\alpha_n))$ and $(\mathrm{W}^v(\alpha))$,

$$\begin{aligned} (16) \qquad \|\mathbf{u}_n-\mathbf{u}\|^2_{\mathbf{curl},\Omega} &\leqslant \mu_1 C_1^2 a_{\alpha_n}(\mathbf{u}_n-\mathbf{u},\mathbf{u}_n-\mathbf{u}) \\ &= \mu_1 C_1^2 (f^v(\mathbf{u}_n-\mathbf{u}) - a_{\alpha_n}(\mathbf{u}_n-\mathbf{u},\mathbf{u})) \\ &= \mu_1 C_1^2 (a_\alpha(\mathbf{u}_n-\mathbf{u},\mathbf{u}) - a_{\alpha_n}(\mathbf{u}_n-\mathbf{u},\mathbf{u})). \end{aligned}$$

Further, we denote the characteristic functions of the sets $\Omega_0(\alpha)$ and $\Omega_1(\alpha)$ by $\chi_0(\mathbf{x},\alpha)$ and $\chi_1(\mathbf{x},\alpha)$, respectively. Since $\alpha_n\rightrightarrows\alpha$, we have

$$(17) \qquad \chi_0(\mathbf{x},\alpha_n)\to\chi_0(\mathbf{x},\alpha) \text{ and } \chi_1(\mathbf{x},\alpha_n)\to\chi_1(\mathbf{x},\alpha) \text{ a.e. in } \Omega \text{ as } n\to\infty.$$

Now, using the Cauchy-Schwarz inequality in $[L^2(\Omega)]^3$ yields

$$
\begin{aligned}
(18)\quad & |a_\alpha(\mathbf{u}_n - \mathbf{u}, \mathbf{u}) - a_{\alpha_n}(\mathbf{u}_n - \mathbf{u}, \mathbf{u})| \\
&= \frac{1}{\mu_0} \int_\Omega \{(\chi_0(\mathbf{x}, \alpha) - \chi_0(\mathbf{x}, \alpha_n))\mathbf{curl}(\mathbf{u})\} \cdot \mathbf{curl}(\mathbf{u}_n - \mathbf{u})\, \mathrm{d}\mathbf{x} \\
&\quad + \frac{1}{\mu_1} \int_\Omega \{(\chi_1(\mathbf{x}, \alpha) - \chi_1(\mathbf{x}, \alpha_n))\mathbf{curl}(\mathbf{u})\} \cdot \mathbf{curl}(\mathbf{u}_n - \mathbf{u})\, \mathrm{d}\mathbf{x} \\
&\leqslant \frac{1}{\mu_0} (\|(\chi_0(\mathbf{x}, \alpha) - \chi_0(\mathbf{x}, \alpha_n))\mathbf{curl}(\mathbf{u})\|_{[L^2(\Omega)]^3} \\
&\quad + \|(\chi_1(\mathbf{x}, \alpha) - \chi_1(\mathbf{x}, \alpha_n))\mathbf{curl}(\mathbf{u})\|_{[L^2(\Omega)]^3}) \cdot \|\mathbf{curl}(\mathbf{u}_n - \mathbf{u})\|_{[L^2(\Omega)]^3}.
\end{aligned}
$$

From (17), for $i = 0, 1$, $|\chi_i(\mathbf{x}; \alpha) - \chi_i(\mathbf{x}; \alpha_n)|^2 \|\mathbf{curl}(\mathbf{u}(\mathbf{x}))\|^2 \to 0$ a.e. Ω as $n \to \infty$. Now, by the Lebesgue dominated convergence theorem, cf. [21, p. 26], the right-hand side of (18) tends to zero. Together with (16) this completes the proof. □

3.3. Shape optimization problem

Let $\mathcal{I}\colon \mathcal{U} \times [\mathbf{H_0}(\mathbf{curl}; \Omega)]^{n_\mathrm{v}} \mapsto \mathbb{R}$ be a continuous functional. Using $(\mathrm{W}^v(\alpha))$, we define the cost functional $\mathcal{J}\colon \mathcal{U} \mapsto \mathbb{R}$ by $\mathcal{J}(\alpha) := \mathcal{I}(\alpha, \mathbf{u}^1(\alpha), \ldots, \mathbf{u}^{n_\mathrm{v}}(\alpha))$. The continuous optimization problem is then formulated as follows:

$$
(\mathrm{P}) \qquad \begin{cases} \text{Find } \alpha^* \in \mathcal{U}\colon \\ \mathcal{J}(\alpha^*) \leqslant \mathcal{J}(\alpha) \quad \forall\, \alpha \in \mathcal{U}. \end{cases}
$$

Theorem 1. *There exists $\alpha^* \in \mathcal{U}$ which is a solution to* (P).

P r o o f. By Lemma 7, $\mathcal{U}$ is a compact subset of the normed linear space $C(\overline{\omega})$. Using the continuity of $\mathcal{I}$ and Lemma 8 we obtain the continuity of $\mathcal{J}$ on $\mathcal{U}$. Now the assertion follows from a classical theorem, cf. [11, Th. 1.3]. □

Moreover, we use (14) to define the cost functional $\widetilde{\mathcal{J}}\colon \Upsilon \mapsto \mathbb{R}$ by $\widetilde{\mathcal{J}}(\mathbf{p}) := \mathcal{J}(F(\mathbf{p}))$. Then, by the compactness of Υ, the continuity of F on Υ, and Theorem 1, there exists a solution to the finite-dimensional optimization problem

$$
(\widetilde{\mathrm{P}}) \qquad \begin{cases} \text{Find } \mathbf{p}^* \in \Upsilon\colon \\ \widetilde{\mathcal{J}}(\mathbf{p}^*) \leqslant \widetilde{\mathcal{J}}(\mathbf{p}) \ \ \forall\, \mathbf{p} \in \Upsilon. \end{cases}
$$

3.4. Regularization of the bilinear form

Similarly to Section 2.4, the regularized weak formulation reads as follows:

$$
(\mathrm{W}^v_\varepsilon(\alpha)) \qquad \begin{cases} \text{Find } \mathbf{u}^v_\varepsilon(\alpha) \in \mathbf{H_0}(\mathbf{curl}; \Omega)\colon \\ a_{\varepsilon,\alpha}(\mathbf{v}, \mathbf{u}^v_\varepsilon(\alpha)) = f^v(\mathbf{v}) \quad \forall\, \mathbf{v} \in \mathbf{H_0}(\mathbf{curl}; \Omega), \end{cases}
$$

where $a_{\varepsilon,\alpha}(\mathbf{v},\mathbf{u}) := a_\alpha(\mathbf{v},\mathbf{u}) + \varepsilon \int_\Omega \mathbf{v}\cdot\mathbf{u}\,\mathrm{d}\mathbf{x}$. The corresponding shape optimization problem reads

$$(\mathrm{P}_\varepsilon) \qquad \begin{cases} \text{Find } \alpha_\varepsilon{}^* \in \mathcal{U}: \\ \mathcal{J}_\varepsilon(\alpha_\varepsilon{}^*) \leqslant \mathcal{J}_\varepsilon(\alpha) \quad \forall\, \alpha \in \mathcal{U}, \end{cases}$$

where $\mathcal{J}_\varepsilon(\alpha) := \mathcal{I}(\alpha, \mathbf{u}_\varepsilon^1(\alpha), \dots, \mathbf{u}_\varepsilon^{n_\mathrm{v}}(\alpha))$. The existence of an optimal solution to (P_ε) can be proven as in Theorem 1.

Theorem 2. *Let $\{\varepsilon_n\}_{n=1}^\infty \subset \mathbb{R}$ be a sequence of positive regularization parameters such that $\varepsilon_n \to 0_+$ as $n \to \infty$, and let $\alpha_{\varepsilon_n}{}^*$ be the corresponding solutions to $(\mathrm{P}_{\varepsilon_n})$. Then there exist a subsequence $\{\varepsilon_{n_k}\}_{k=1}^\infty \subset \{\varepsilon_n\}_{n=1}^\infty$ and a shape $\alpha^* \in \mathcal{U}$ such that*

$$\alpha_{\varepsilon_{n_k}}{}^* \to \alpha^* \quad \text{in } \mathcal{U} \text{ as } k \to \infty$$

holds and, moreover, α^* is a solution to (P).

P r o o f. Here we make use of Lemma 3, see [11] or [17, p. 73]. □

3.5. Finite element approximation

Let $h > 0$ be a discretization parameter as in Section 2.5. Referring to Fig. 3 we will introduce a finite-dimensional approximation of $\mathcal{U}$. Let $\mathcal{T}_\omega^h := \{\omega_1^h, \dots, \omega_{n_\omega^h}^h\}$, where $n_\omega^h \in \mathbb{N}$, be a triangulation of a rectangular domain ω. Let $P^1(\mathcal{T}_\omega^h)$ denote the space of continuous functions that are linear over each $\overline{\omega_i^h}$. Then the discretized set of admissible shapes is

$$\mathcal{U}^h := \{\alpha^h \in P^1(\mathcal{T}_\omega^h) \mid \forall\, \mathbf{x},\mathbf{y} \in \overline{\omega}\colon\ |\alpha^h(\mathbf{x}) - \alpha^h(\mathbf{y})| \leqslant C_5\|\mathbf{x}-\mathbf{y}\| \text{ and } \alpha_\mathrm{l} \leqslant \alpha^h(\mathbf{x}) \leqslant \alpha_\mathrm{u}\}.$$

The set $\mathcal{U}^h$ is clearly finite-dimensional and closed, and thus, compact. Let $\pi_\omega^h\colon \mathcal{U} \mapsto P^1(\mathcal{T}_\omega^h)$ interpolate shapes at the nodes of $\mathcal{T}_\omega^h$. Then, as in [1],

$$(19) \qquad \forall\, \alpha \in \mathcal{U}\colon\ \pi_\omega^h(\alpha) \rightrightarrows \alpha \text{ as } h \to 0_+.$$

Again, given a discretized shape α^h, we consider the decomposition of Ω into $\Omega_0(\alpha^h)$ and $\Omega_1(\alpha^h)$, an example of which is depicted in Fig. 3. We provide a discretization $\mathcal{T}^h(\alpha^h) := \{K^{e_1}(\alpha^h), \dots, K^{e_{n_\Omega}}(\alpha^h)\}$ of Ω such that

$$\forall\, K^{e_i}(\alpha^h) \in \mathcal{T}^h(\alpha^h)\colon\ K^{e_i}(\alpha^h) \subset \Omega_0(\alpha^h) \text{ or } K^{e_i}(\alpha^h) \subset \Omega_1(\alpha^h).$$

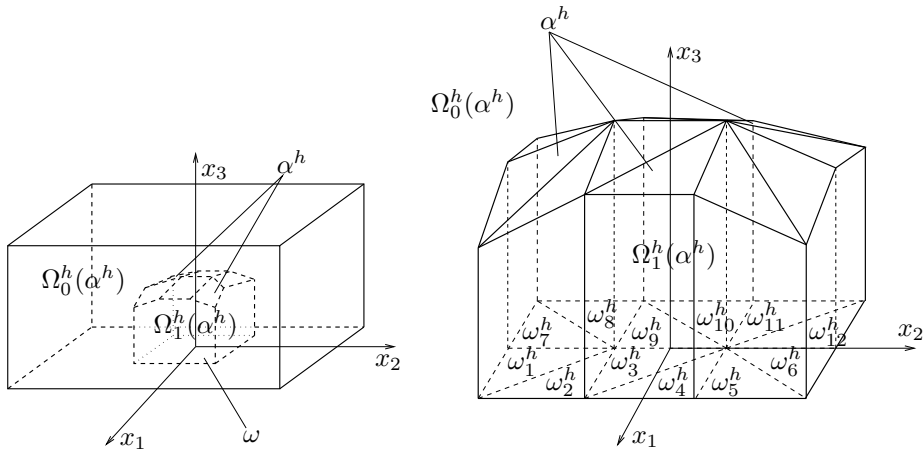

Figure 3. Decomposition of Ω^h.

Assumption 2. We assume that for any $h > 0$ fixed ($h \leqslant \overline{h}$) the connectivity of the discretization grid $\mathcal{T}^h(\alpha^h)$ is independent of α^h, we further assume that the corners $\mathbf{x}_1^{e_i}(\alpha^h), \ldots, \mathbf{x}_4^{e_i}(\alpha^h)$ of $K^{e_i}(\alpha^h)$ form a tetrahedron and they depend continuously on α^h.

The regularized and discretized multistate problem is

$$(\mathrm{W}_\varepsilon^{v,h}(\alpha^h)) \qquad \begin{cases} \text{Find } \mathbf{u}_\varepsilon^{v,h}(\alpha^h) \in \mathbf{H_0}(\mathbf{curl}; \Omega; \alpha^h)^h : \\ a_{\varepsilon,\alpha^h}(\mathbf{v}^h, \mathbf{u}_\varepsilon^{v,h}(\alpha^h)) = f^v(\mathbf{v}^h) \quad \forall\, \mathbf{v}^h \in \mathbf{H_0}(\mathbf{curl}; \Omega; \alpha^h)^h. \end{cases}$$

The existence of a unique solution to $(\mathrm{W}_\varepsilon^{v,h}(\alpha^h))$ is easy to prove.

Lemma 9. *For each $v = 1, \ldots, n_{\mathrm{v}}$, $\varepsilon > 0$ and $h > 0$ ($h \leqslant \overline{h}$) the mapping $\mathbf{u}_\varepsilon^{v,h} : \mathcal{U}^h \mapsto \mathbf{H_0}(\mathbf{curl}; \Omega)$ is continuous.*

P r o o f. Now we cannot use the same technique as in the proof of Lemma 8, since the settings $(\mathrm{W}_\varepsilon^{v,h}(\alpha^h))$ differ from $\alpha^h \in \mathcal{U}^h$. Therefore, the estimate (16) cannot be established. Instead, we have to exploit the algebraic structure of the mapping $\mathbf{u}_\varepsilon^{v,h}$. The proof is given in [17, p. 77]. □

Lemma 10. *Let $\varepsilon > 0$, $\{h_n\}_{n=1}^\infty \subset \mathbb{R}$, $0 < h_n \leqslant \overline{h}$, be such that $h_n \to 0_+$ as $n \to \infty$, and let $\alpha \in \mathcal{U}$, $\{\alpha^{h_n}\}_{n=1}^\infty \subset \mathcal{U}$, $\alpha^{h_n} \in \mathcal{U}^{h_n}$, be such that $\alpha^{h_n} \to \alpha$ in $\mathcal{U}$ as $n \to \infty$. Then for each $v = 1, \ldots, n_{\mathrm{v}}$ we have*

$$\mathbf{u}_\varepsilon^{v,h_n}(\alpha^{h_n}) \to \mathbf{u}_\varepsilon^v(\alpha) \text{ in } \mathbf{H_0}(\mathbf{curl}; \Omega) \text{ as } n \to \infty,$$

where $\mathbf{u}_\varepsilon^{v,h_n}(\alpha^{h_n})$ is the solution to $(\mathrm{W}_\varepsilon^{v,h_n}(\alpha^{h_n}))$ and $\mathbf{u}_\varepsilon^v(\alpha)$ solves $(\mathrm{W}_\varepsilon^v(\alpha))$.

P r o o f. It is enough to prove that the assumption (8) is fulfilled and the rest follows from Lemma 6. We specify $\mu(\mathbf{x}) \equiv \mu_\alpha(\mathbf{x})$ and $\mu^{h_n}(\mathbf{x}) \equiv \mu_{\alpha^{h_n}}(\mathbf{x})$, where

$$\mu_\alpha(\mathbf{x}) := \begin{cases} \mu_0, & \mathbf{x} \in \Omega_0(\alpha), \\ \mu_1, & \mathbf{x} \in \Omega_1(\alpha), \end{cases} \qquad \alpha \in \mathcal{U}.$$

Let us take an arbitrary point $\mathbf{x} \in \Omega_0(\alpha) \cup \Omega_1(\alpha)$. We suppose that $\mathbf{x} \in \Omega_0(\alpha)$, i.e., $\mu_\alpha(\mathbf{x}) = \mu_0$ while the other case is an analogue. Since $\alpha^{h_n} \rightrightarrows \alpha$ for $n \to \infty$, there exists $n_0 \in \mathbb{N}$ such that $\mathbf{x} \in \Omega_0(\alpha^{h_n})$ for all $n \geqslant n_0$, thus, $\mu_{\alpha^{h_n}}(\mathbf{x}) = \mu_\alpha(\mathbf{x}) = \mu_0$ and the proof is complete. □

The relevant setting of the shape optimization problem reads

$$(\mathrm{P}_\varepsilon^h) \qquad \begin{cases} \text{Find } \alpha_\varepsilon^{h\,*} \in \mathcal{U}^h\colon \\ \mathcal{J}_\varepsilon^h(\alpha_\varepsilon^{h\,*}) \leqslant \mathcal{J}_\varepsilon^h(\alpha^h) \quad \forall\, \alpha^h \in \mathcal{U}^h, \end{cases}$$

where $\mathcal{J}_\varepsilon^h(\alpha^h) := \mathcal{I}(\alpha^h, \mathbf{u}_\varepsilon^{1,h}(\alpha^h), \dots, \mathbf{u}_\varepsilon^{n_\mathrm{v},h}(\alpha^h))$. The existence theorem holds.

Theorem 3. *Let $\varepsilon > 0$, let $\{h_n\}_{n=1}^\infty \subset \mathbb{R}$, $0 < h_n \leqslant \overline{h}$, be such that $h_n \to 0_+$ as $n \to \infty$, and let $\alpha_\varepsilon^{h_n\,*} \in \mathcal{U}^{h_n}$ denote the corresponding solutions to $(\mathrm{P}_\varepsilon^{h_n})$. Then there exist a subsequence $\{h_{n_k}\}_{k=1}^\infty \subset \{h_n\}_{n=1}^\infty$ and a shape $\alpha_\varepsilon{}^* \in \mathcal{U}$ such that*

$$\alpha_\varepsilon^{h_{n_k}\,*} \to \alpha_\varepsilon{}^* \text{ in } \mathcal{U} \quad \text{as } k \to \infty$$

holds and, moreover, $\alpha_\varepsilon{}^*$ is a solution to the problem (P_ε).

P r o o f. By Lemma 7, there exist a subsequence of optimized shapes $\{\alpha_\varepsilon^{h_{n_k}\,*}\}_{k=1}^\infty \subset \{\alpha_\varepsilon^{h_n\,*}\}_{n=1}^\infty$ and a shape $\alpha_\varepsilon{}^* \in \mathcal{U}$ such that

$$\alpha_\varepsilon^{h_{n_k}\,*} \to \alpha_\varepsilon{}^* \text{ in } \mathcal{U} \quad \text{as } k \to \infty. \tag{20}$$

Let $\alpha \in \mathcal{U}$ be an arbitrary shape. For any $k \in \mathbb{N}$, by the definition of $(\mathrm{P}_\varepsilon^{h_{n_k}})$ and since $\pi_\omega^{h_{n_k}}(\alpha) \in \mathcal{U}^{h_{n_k}}$, we have

$$\mathcal{J}_\varepsilon^{h_{n_k}}(\alpha_\varepsilon^{h_{n_k}\,*}) \leqslant \mathcal{J}_\varepsilon^{h_{n_k}}(\pi_\omega^{h_{n_k}}(\alpha)). \tag{21}$$

Using (19) or (20), Lemma (10), and the continuity of $\mathcal{I}$, the right- or left-hand side of (21) respectively converges to $\mathcal{J}_\varepsilon(\alpha)$ or $\mathcal{J}_\varepsilon(\alpha_\varepsilon{}^*)$ as $k \to \infty$. □

Finally, we introduce the regularized and discretized cost functional $\widetilde{\mathcal{J}}_\varepsilon^h\colon\ \Upsilon \mapsto \mathbb{R}$ by $\widetilde{\mathcal{J}}_\varepsilon^h(\mathbf{p}) := \mathcal{J}_\varepsilon^h(\pi_\omega^h(F(\mathbf{p})))$. The related optimization problem is

$$(\widetilde{\mathrm{P}}_\varepsilon^h) \qquad \begin{cases} \text{Find } \mathbf{p}_\varepsilon^{h\,*} \in \Upsilon\colon \\ \widetilde{\mathcal{J}}_\varepsilon^h(\mathbf{p}_\varepsilon^{h\,*}) \leqslant \widetilde{\mathcal{J}}_\varepsilon^h(\mathbf{p}) \quad \forall\, \mathbf{p} \in \Upsilon. \end{cases}$$

R e m a r k 1. In cases of complex geometries, as that in Section 4, Assumption 2 is a serious bottleneck of this discretization approach. For small discretization parameters and large changes in the design we cannot guarantee that the perturbed elements still satisfy the regularity condition. They might be even flipped. In this case, we have to re-mesh the geometry and solve the optimization problem again, but now on a grid of different topology. Then certainly the cost functional is not continuous any more and the just introduced convergence theory cannot be applied. Nevertheless, in literature this approach is still the most frequently used one as far as a finite element discretization is concerned. In practice, after we get an optimized shape we should compare the value of a very fine discretized cost functional for the optimized design with the value of the initial one. If we can see a progress then the optimization surely did a good job. Some solutions to this inconsistency between the theory and practice are discussed in Conclusions.

3.6. Sensitivity analysis

We will solve $(\widetilde{\mathrm{P}}_\varepsilon^h)$ by sequential quadratic programming with an updating formula of the Hessian matrix. To this end we have to provide the gradient of the cost functional $\widetilde{\mathcal{J}}_\varepsilon^h$ with respect to the design parameters $\mathbf{p}$. Let us note that the gradient of the constraint functional $\boldsymbol{v}^h\colon\ \mathbb{R}^{n_\Upsilon} \mapsto \mathbb{R}^{n_{\boldsymbol{v}^h}}$, where $n_{\boldsymbol{v}^h} \in \mathbb{N}$, which is defined so that

$$\Upsilon = \{\mathbf{p} \in \mathbb{R}^{n_\Upsilon} \mid \boldsymbol{v}^h(\mathbf{p}) \leqslant \mathbf{0}\}$$

can be easily calculated by hand. The evaluation of the cost functional proceeds as follows:

$$\mathbf{p} \xrightarrow{\pi_\omega^h \circ F} \boldsymbol{\alpha}^h \xrightarrow{\boldsymbol{K}^h \cdot \triangle \mathbf{x}^h = \boldsymbol{b}^h(\boldsymbol{\alpha}^h)} \mathbf{x}^h \xrightarrow{\text{FEM}} \boldsymbol{A}_\varepsilon^n, \boldsymbol{f}^{v,n} \xrightarrow{\boldsymbol{A}_\varepsilon^n \cdot \boldsymbol{u}_\varepsilon^{v,n} = \boldsymbol{f}^{v,n}}$$
$$\xrightarrow{\boldsymbol{A}_\varepsilon^n \cdot \boldsymbol{u}_\varepsilon^{v,n} = \boldsymbol{f}^{v,n}} \boldsymbol{u}_\varepsilon^{v,n} \xrightarrow{\mathcal{I}^h(\boldsymbol{\alpha}^h, \mathbf{x}^h, \boldsymbol{u}_\varepsilon^{1,n_\Omega}, \ldots, \boldsymbol{u}_\varepsilon^{n_\mathrm{v},n_\Omega})} \widetilde{\mathcal{J}}_\varepsilon^h(\mathbf{p}),$$

where the shape-to-mesh mapping

$$\boldsymbol{K}^h \cdot \triangle \mathbf{x}^h(\boldsymbol{\alpha}^h) = \boldsymbol{b}^h(\boldsymbol{\alpha}^h)$$

maps the shape nodal coordinates $\boldsymbol{\alpha}^h$ onto the remaining nodal coordinates $\mathbf{x}^h$ in the grid. It is based on solving an auxiliary discretized 3d linear elasticity problem

in terms of grid displacements $\triangle \mathbf{x}^h(\boldsymbol{\alpha}^h)$ with a nonhomogeneous Dirichlet boundary condition that corresponds to the given shape displacements $\boldsymbol{\alpha}^h$, and with zero displacements on $\partial\Omega$ and on the boundaries of the subdomains with nonzero current density $\mathbf{J}^v$. Here, $\boldsymbol{K}^h \equiv \boldsymbol{K}^h(\mathbf{x}_0^h)$ is a nonsingular stiffness matrix assembled on the initial grid $\mathbf{x}_0^h$ and $\boldsymbol{b}^h(\boldsymbol{\alpha}^h)$ is the right-hand side vector linearly dependent on $\boldsymbol{\alpha}^h$. The resulting mesh is then calculated by

$$\mathbf{x}^h(\boldsymbol{\alpha}^h) := \mathbf{x}_0^h + \triangle \mathbf{x}^h(\boldsymbol{\alpha}^h) + \boldsymbol{M}^h(\boldsymbol{\alpha}^h),$$

where $\boldsymbol{M}^h \colon \mathbb{R}^{3n_{\boldsymbol{\alpha}^h}} \mapsto \mathbb{R}^{3n_{\mathbf{x}^h}}$ identically maps the nodal coordinates of the shape α^h onto the corresponding coordinates in the grid vector $\mathbf{x}^h$.

We can guarantee the smoothness of $\widetilde{\mathcal{J}}_\varepsilon^h$ via the smoothness of its individual submappings, see [17, p. 87]. Then we are justified to use a Newton-like algorithm.

Concerning the gradient of the cost functional, we use the chain rule to differentiate the cost functional. Then, we apply the adjoint method which evaluates the resulting expression from right to left. Since there is no state dependent constraint, the adjoint method involves only n_{v} additional solutions of the state systems $\boldsymbol{A}_\varepsilon^n$ with the right-hand sides $\mathbf{grad}_{\boldsymbol{u}_\varepsilon^{v,n}}(\mathcal{I}^h)$. Moreover, we have to assemble the derivatives of the element matrices with respect to the grid nodal displacements. They mainly involve derivatives of the matrix $\mathbf{R}^e$ and of its determinant, see (5). The computational effort is comparable to the assembling of the system matrix. The multistate problem sensitivity is then aggregated for each state as follows:

$$\sum_{v=1}^{n_{\mathrm{v}}} \left[-\frac{\partial \boldsymbol{A}_\varepsilon^n}{\partial [\mathbf{x}_1^h]_1} \cdot \boldsymbol{u}_\varepsilon^{v,n}, \ldots, -\frac{\partial \boldsymbol{A}_\varepsilon^n}{\partial [\mathbf{x}_{n_{\mathbf{x}^h}}^h]_3} \cdot \boldsymbol{u}_\varepsilon^{v,n} \right]^T \cdot (\boldsymbol{A}_\varepsilon^n)^{-1} \cdot \mathbf{grad}_{\boldsymbol{u}_\varepsilon^{v,n}}(\mathcal{I}^h).$$

In [17], [19] we develop an efficient object-oriented implementation for shape sensitivity analysis governed by various linear elliptic 2nd-order partial differential equations, where the only part which has always to be recoded by a user is the formula for $\mathcal{I}^h$.

4. An application

4.1. Physical problem

We consider an electromagnet of the Maltese Cross (MC) geometry, as depicted in Fig. 4. It consists of a ferromagnetic yoke and 4 poles completed with coils which are pumped with direct electric currents.

The electromagnets are used for measurements of Kerr magnetooptic effects [31]. The latter are measured by a reflection of an optical beam on a sample located in the

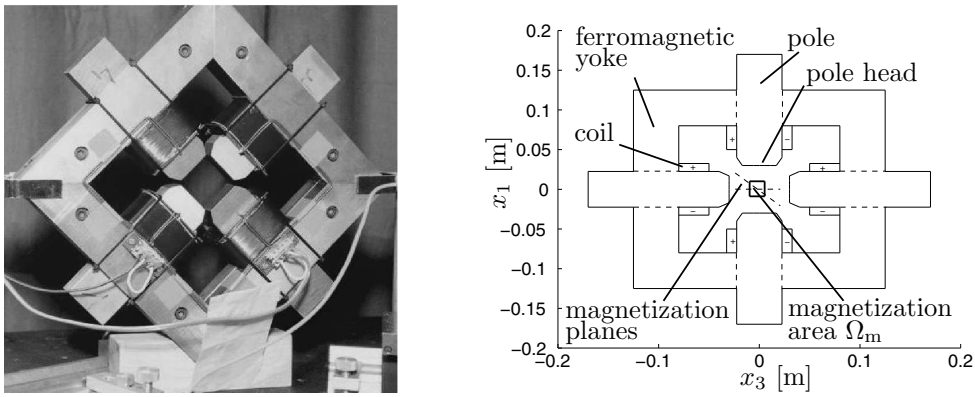

Figure 4. The Maltese Cross electromagnet and its cross-section.

magnetization area Ω_{m}. Here the magnetic field is required to be as homogeneous, i.e., as constant as possible in a given normal direction. Due to the anisotropy the measurements should be done in more directions, see [13], [24], [25]. Therefore, the MC electromagnet is capable of generating magnetic fields homogeneous in up to 8 directions just by switching some currents in coils on or off, or by switching their senses. Our aim is to improve the current geometry of the pole heads of the MC electromagnet such that inhomogeneities of the magnetic field are minimized, but the field itself is still strong enough.

4.2. Mathematical settings

4.2.1. Set of admissible shapes

The geometry of the MC electromagnet is depicted in Fig. 4. The dimensions are in meters. The computational domain is $\Omega := (-0.2, 0.2) \times (-0.05, 0.05) \times (-0.2, 0.2)$. We assume all the pole heads to be the same and symmetric. Then, it is enough to consider the shape α to be a quarter of the shape of the left pole head, while the symmetry with respect to the planes $x_1 = 0$ and $x_2 = 0$ will be involved in the parametrization F later on. The shape is a continuous function defined over $\omega := (0, d_{\mathrm{pole},1}/2) \times (0, d_{\mathrm{pole},2}/2)$, where $d_{\mathrm{pole},1} := 0.045$, $d_{\mathrm{pole},2} := 0.025$. Further, we choose $C_5 := \arctan(3\pi/8)$ and specify the box constraints by $\alpha_{\mathrm{l}} := 0.012$, $\alpha_{\mathrm{u}} := 0.05$. The pole heads cannot penetrate then. Now, the set of admissible shapes $\mathcal{U}$ is determined and Lemma 7 holds.

From the practical point of view, we cannot manufacture any shape, so we consider a Bézier patch of a fixed number of design parameters $n_\Upsilon := n_{\Upsilon,1} \cdot n_{\Upsilon,2}$, where $n_{\Upsilon,1} := 4$, $n_{\Upsilon,2} := 3$. To this end, we decompose the shape domain ω into $(n_{\Upsilon,1} - 1) \cdot (n_{\Upsilon,2} - 1)$ regular rectangles whose $n_{\Upsilon,1} \cdot n_{\Upsilon,2}$ corners are $\mathbf{x}_{\omega,i,j} := ((i-1)d_{\mathrm{pole},1}/(n_{\Upsilon,1}-1), (j-1)d_{\mathrm{pole},2}/(n_{\Upsilon,2}-1))$ for $i = 1, \ldots, n_{\Upsilon,1}$, $j = 1, \ldots, n_{\Upsilon,2}$.

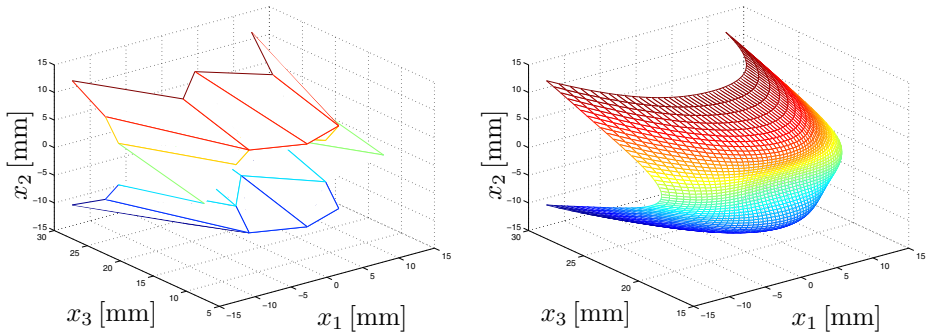

Figure 5. Bézier design parameters and the corresponding shape.

The set Υ is defined as

$$\Upsilon := \{\mathbf{p} := (p_{1,1}, \ldots, p_{n_{\Upsilon,1},n_{\Upsilon,2}}) \in \mathbb{R}^{n_\Upsilon} \mid \alpha_\mathrm{l} \leqslant p_{i,j} \leqslant \alpha_\mathrm{u}\}.$$

The mapping $F\colon \Upsilon \mapsto \mathcal{U}$, see also (14), is the following (tensor product) *Bézier mapping* that involves the symmetry assumed above:

$$\begin{aligned}\alpha(x_1, x_2) &:= [F(x_1, x_2)](\mathbf{p}) \\ &:= \sum_{i=1}^{n_{\Upsilon,1}} \sum_{j=1}^{n_{\Upsilon,2}} p_{i,j} \left[\beta_i^{2n_{\Upsilon,1}-1}\Big(\frac{-2x_1 + d_{\mathrm{pole},1}}{2d_{\mathrm{pole},1}}\Big) + \beta_i^{2n_{\Upsilon,1}-1}\Big(\frac{2x_1 + d_{\mathrm{pole},1}}{2d_{\mathrm{pole},1}}\Big)\right] \\ &\quad \times \left[\beta_j^{2n_{\Upsilon,2}-1}\Big(\frac{-2x_2 + d_{\mathrm{pole},2}}{2d_{\mathrm{pole},2}}\Big) + \beta_j^{2n_{\Upsilon,2}-1}\Big(\frac{2x_2 + d_{\mathrm{pole},2}}{2d_{\mathrm{pole},2}}\Big)\right],\end{aligned}$$

where $(x_1, x_2) \in \overline{\omega}$ and where for $n \in \mathbb{N}$, $i \in \mathbb{N}$, $i \leqslant n$, and $t \in [0, 1]$ we have

$$\beta_i^n(t) := \frac{(n-1)!}{(i-1)!\,(n-i)!} t^{i-1}(1-t)^{n-i},$$

which is called the *Bernstein polynomial*. An example of the mapping F is depicted in Fig. 5. Concerning 15, we perform the mirroring of the shape α with respect to the planes $x_1 = 0$ and $x_2 = 0$ and, moreover, copy this resulting shape to all the remaining pole heads. In this way the shape α controls the decomposition of Ω into $\Omega_0(\alpha)$ that denotes the domain occupied by the coils or air and into $\Omega_1(\alpha)$ which is the domain occupied by the yoke or poles. It is easy to see that the mapping F is continuous on Υ.

4.2.2. Multistate problem

Concerning the bilinear form, $\mu_0 := 4\pi 10^{-7}\,[\mathrm{Hm}^{-1}]$ is the air permeability and $\mu_1 := 5100\mu_0\,[\mathrm{Hm}^{-1}]$ is the permeability of the kind of steel used. We distinguish

two variations of $\mathbf{J}^v$, namely, we set $v := 1$ for a vertical variation for which only two opposite coils are pumped and $v := 2$ for a diagonal variation for which four coils are pumped as in Fig. 4. Each of the other 6 variations of the current excitation is given by a mirroring. We consider the static current $I = 5\,[\mathrm{A}]$ and 600 turns on each coil. The compatibility condition (3) is obviously fulfilled.

4.2.3. Shape optimization problem

We introduce the magnetization area $\Omega_{\mathrm{m}} := (-0.005, 0.005)^3$, see Fig. 4. The cost functional is

$$\mathcal{I}(\mathbf{u}^1(\alpha,\mathbf{x}), \mathbf{u}^2(\alpha,\mathbf{x})) := \frac{1}{2} \cdot \sum_{v=1}^{2} [\varphi^v(\mathbf{B}^v(\alpha,\mathbf{x})) + \varrho \cdot \theta^v(\mathbf{B}^v(\alpha,\mathbf{x}))],$$

where, for $v = 1, 2$, $\mathbf{B}^v(\alpha,\mathbf{x}) := \mathbf{curl}_{\mathbf{x}}(\mathbf{u}^v(\alpha,\mathbf{x}))$ is the magnetic field of the vth state problem, and where the particular contributions are defined by

$$\begin{aligned}
\varphi^v(\mathbf{B}^v(\alpha,\mathbf{x})) &:= \frac{1}{\mathrm{meas}(\Omega_{\mathrm{m}}) \cdot (B_{\min}^{\mathrm{avg},v})^2} \\
&\quad \times \int_{\Omega_{\mathrm{m}}} \|\mathbf{B}^v(\alpha,\mathbf{x}) - B^{\mathrm{avg},v}(\mathbf{B}^v(\alpha,\mathbf{x})) \cdot \mathbf{n}_{\mathrm{m}}^v\|^2 \,\mathrm{d}\mathbf{x}, \\
\theta^v(\mathbf{B}^v(\alpha,\mathbf{x})) &:= (\max\{0, B_{\min}^{\mathrm{avg},v} - B^{\mathrm{avg},v}(\mathbf{B}^v(\alpha,\mathbf{x}))\})^2, \quad \varrho := 10^6, \\
B^{\mathrm{avg},v}(\mathbf{B}^v(\alpha,\mathbf{x})) &:= \frac{1}{\mathrm{meas}(\Omega_{\mathrm{m}})} \cdot \int_{\Omega_{\mathrm{m}}} \|\mathbf{B}^v(\alpha,\mathbf{x}) \cdot \mathbf{n}_{\mathrm{m}}^v\| \,\mathrm{d}\mathbf{x},
\end{aligned}$$

where $B_{\min}^{\mathrm{avg},1} = B_{\min}^{\mathrm{avg},2} := 0.08\,[\mathrm{T}]$, $\mathbf{n}_{\mathrm{m}}^1 := (1,0,0)$, and $\mathbf{n}_{\mathrm{m}}^2 := (1/\sqrt{2}, 0, 1/\sqrt{2})$. It is obvious that $\mathcal{I}$ is continuous. Now the existence of solutions to both the problems (P) and $(\widetilde{\mathrm{P}})$ follows.

Further, we choose $\varepsilon := 10^{-6}$ and $\overline{h} := 0.4$. The triangulation $\mathcal{T}_\omega^h$ of the shape domain involves the nodes $\mathbf{x}_{\omega,i,j}$. The integrals involved in the cost functional are replaced by the corresponding sums over elements.

4.3. Numerical results

The problem is solved using scientific software tools [15], [19], [28]. They have been developed within SFB F013 at the University of Linz, Austria. The resulting linear systems are solved by a preconditioned conjugate gradient method. In case the number of design variables is small, a direct solver is applied. Concerning optimization, we use the sequential quadratic programming (SQP) with an updating formulae of the Hessian matrix. The gradient is calculated by the adjoint method. Moreover, we have introduced and used a multilevel optimization approach the idea of which is to use the SQP within a hierarchy of discretizations of the optimization problem such

that a coarse optimized design is prolonged and used as the initial guess at the next finer level. In [20] we have shown that using the multilevel approach significantly reduces the computational time.

The 3d optimized shape is described by 12 design variables and was solved in 93 SQP iterations which took almost 30 hours. The underlying discretized 3d state problem has 29541 unknowns. The 2d and 3d resulting shapes are depicted in Fig. 6, where the reduced 2d problem has arisen by neglecting the dimension x_2. The initial design is depicted in Fig. 4. Some 2d and preliminary 3d numerical results, as well as various details, are presented in [16], [18].

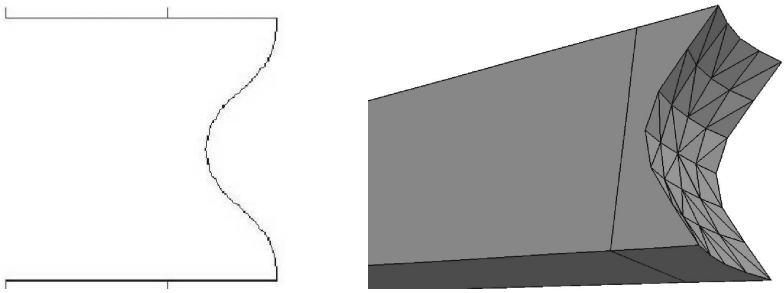

Figure 6. 2d and 3d optimized pole heads of the MC electromagnet.

4.4. Manufacture and measurements

After the 2d optimized shape, see Fig. 6, the pole heads were manufactured and the magnetic field was measured. In Fig. 7 the related distributions of the normal component of the magnetic flux density are depicted. We can see a significant improvement of the homogeneity of the magnetic field. The cost functional calculated from the measured data decreased 4.5-times. Nevertheless, the magnitude of the magnetic field decreased as well. Choosing a proper compromise between the homogeneity and the strength of the magnetic field is a difficult engineering task. Moreover, the relative differences between the measured and the calculated magnetic fields are about 30 %, which might be caused by saturation of the magnetic field in the corners. Employing a nonlinear governing magnetostatic state problem should improve this mismatch.

5. Conclusions

This paper treated the shape optimization in three-dimensional linear magnetostatics. We have met one serious obstacle, see Remark 1, that we can hardly find a continuous mapping between the shape design nodes and the remaining nodes in the discretization grid. For fine discretizations and large changes in the design shape

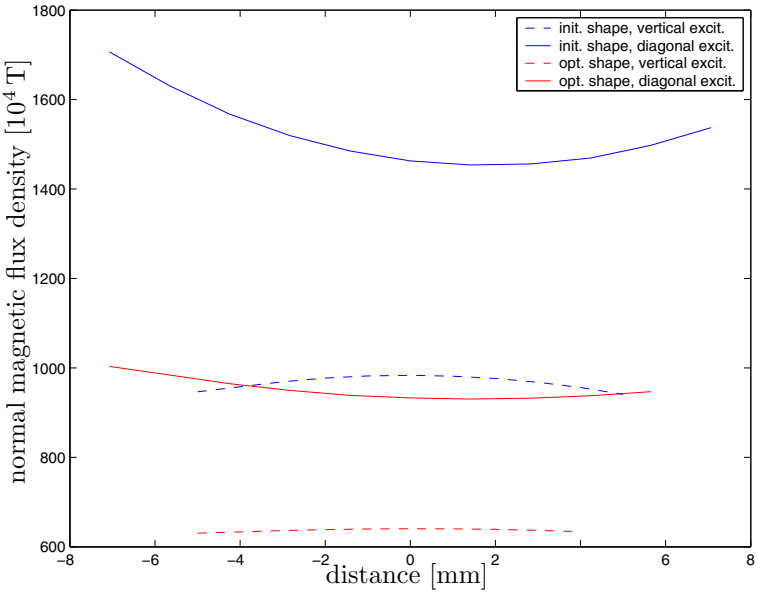

Figure 7. Magnetic field for the initial and the optimized design.

some elements flip. One possible solution consists in the use of the multilevel optimization techniques, where on the fine grids the difference between the initial and optimized shapes is not that big. Another one might be when using composite finite elements that were developed for the treatment with complicated geometries in the papers [8], [9]. It is also connected to fictitious domain methods, cf. [10]. We can also avoid this problem by using a boundary element discretization. However, construction of efficient multigrid solvers as well as using the method for nonlinear governing state problems are still topics of the current research.

References

[1] *D. Begis, R. Glowinski*: Application de la méthode des éléments finis à la résolution d'un problème de domaine optimal. Méthodes de résolution des problèmes. Appl. Math. Optim. *2* (1975), 130–169. (In French.)

[2] *A. Bossavit*: Computational Electromagnetism. Variational Formulations, Complementarity, Edge Elements. Academic Press, Orlando, 1998.

[3] *D. Braess*: Finite Elements. Theory, Fast Solvers, and Applications in Solid Mechanics. Cambridge University Press, Cambridge, 2001.

[4] *J. Chleboun, R. Mäkinen*: Primal hybrid formulation of an elliptic equation in smooth optimal shape problems. Adv. Math. Sci. Appl. *5* (1995), 139–162.

[5] *P. Doktor*: On the density of smooth functions in certain subspaces of Sobolev spaces. Comment. Math. Univ. Carolin. *14* (1973), 609–622.

[6] *G. E. Farin*: Curves and Surfaces for Computer-Aided Geometric Design: A Practical Guide. Academic Press, Boston, 1997.

[7] *V. Girault, P.-A. Raviart*: Finite Element Methods for Navier-Stokes equations. Theory and Algorithms. Springer-Verlag, Berlin, 1986.

[8] *W. Hackbusch, S. A. Sauter*: Composite finite elements for the approximation of PDEs on domains with complicated micro-structures. Numer. Math. *75* (1997), 447–472.

[9] *W. Hackbusch, S. A. Sauter*: Composite finite elements for problems containing small geometric details. II: Implementation and numerical results. Comput. Vis. Sci. *1* (1997), 15–25.

[10] *J. Haslinger, T. Kozubek*: A fictitious domain approach for a class of Neumann boundary value problems with applications in shape optimization. East-West J. Numer. Math. *8* (2000), 1–23.

[11] *J. Haslinger, P. Neittaanmäki*: Finite Element Approximation for Optimal Shape, Material and Topology Design, 2nd ed. Wiley, Chichester, 1996.

[12] *R. Hiptmair*: Multilevel preconditioning for mixed problems in three dimensions. PhD. thesis. University of Augsburg, 1996.

[13] *I. Kopřiva, D. Hrabovský, K. Postava, D. Ciprian, and J. Pištora*: Anisotropy of the quadratic magneto-optical effects in a cubic crystal. Proceedings of SPIE, Vol. 4016. 2000, pp. 54–59.

[14] *M. Křížek, P. Neittaanmäki*: Mathematical and Numerical Modelling in Electrical Engineering. Theory and Practice. Kluwer Academic Publishers, Dordrecht, 1996.

[15] *M. Kuhn, U. Langer, and J. Schöberl*: Scientific computing tools for 3d magnetic field problems. In: The Mathematics of Finite Elements and Applications. Proceedings of the 10th conference MAFELAP, 1999 (J R. Whiteman, ed.). 2000, pp. 239–258.

[16] *D. Lukáš*: Shape optimization of homogeneous electromagnets. Scientific Computing in Electrical Engineering. Lect. Notes Comput. Sci. Eng. Vol. 18 (U. van Rienen, M. Günther, and D. Hecht, eds.). 2001, pp. 145–152.

[17] *D. Lukáš*: Optimal Shape Design in Magnetostatics. PhD. thesis. VŠB-Technical University, Ostrava, 2003.

[18] *D. Lukáš, I. Kopřiva, D. Ciprian, and J. Pištora*: Shape optimization of homogeneous electromagnets and their application to measurements of magnetooptic effects. Records of COMPUMAG (2001), 156–157.

[19] *D. Lukáš, W. Mühlhuber, and M. Kuhn*: An object-oriented library for the shape optimization problems governed by systems of linear elliptic partial differential equations. Transactions of the VŠB-Technical University Ostrava *1* (2001), 115–128.

[20] *D. Lukáš, D. Ciprian, J. Pištora, K. Postava, and M. Foldyna*: Multilevel solvers for 3-dimensional optimal shape design with an application to magneto-optics. Proceedings of the 9th International Symposium on Microwave and Optical Technology (ISMOT 2003, Ostrava), SPIE Vol. 5445. 2004, pp. 235–239.

[21] *J. Lukeš, J. Malý*: Measure and Integral. MATFYZPRESS, Praha, 1995.

[22] *J. C. Nédélec*: Mixed finite elements in $\mathbb{R}^3$. Numer. Math. *35* (1980), 315–341.

[23] *O. Pironneau*: Optimal Shape Design for Elliptic Systems. Springer Series in Computational Physics. Springer-Verlag, New York, 1984.

[24] *J. Pištora, K. Postava, and R. Šebesta*: Optical guided modes in sandwiches with ultrathin metallic films. Journal of Magnetism and Magnetic Materials *198–199* (1999), 683–685.

[25] *K. Postava, D. Hrabovský, J. Pištora, A. R. Fert, Š. Višňovský, and T. Yamaguchi*: Anisotropy of quadratic magneto-optic effects in reflection. J. Appl. Phys. *91* (2002), 7293–7295.

[26] *P.-A. Raviart and J. M. Thomas*: A mixed finite element method for second order elliptic problems. Lecture Notes in Math. *606* (1977), 292–315.

[27] *S. Reitzinger, J. Schöberl*: An algebraic multigrid method for finite element discretizations with edge elements. Numer. Linear Algebra Appl. *9* (1997), 223–238.
[28] *J. Schöberl*: NETGEN: An advancing front 2D/3D-mesh generator based on abstract rules. Comput. Vis. Sci. *1* (1997), 41–52.
[29] *N. Takahashi*: Optimization of die press model. Proceedings of the TEAM Workshop in the Sixth Round (Okayama, Japan), March 1996.
[30] *U. van Rienen*: Numerical methods in computational electrodynamics. Linear Systems in Practical Applications, Lect. Notes Comp. Sci. Engrg. Vol. 12. Springer-Verlag, Berlin, 2001.
[31] *A. K. Zvedin, V. A. Kotov*: Modern Magnetooptics and Magnetooptical Materials. Institute of Physics Publishing, Bristol and Philadelphia, 1997.

Author's address: *D. Lukáš*, Department of Applied Mathematics (K457), VŠB-Technical University of Ostrava, 17. listopadu 15, 708 33 Ostrava-Poruba, Czech Republic, e-mail: `dalibor.lukas@vsb.cz`.